scientific reports

Check for updates

OPEN

Global-best-guided electric eel foraging optimizer for robust parameter identification of Lorenz and memristive chaotic systems

Davut Izci[1,2]✉, Serdar Ekinci[3], İrfan Ökten[3], Vedat Tümen[3], Burcu Bektaş Güneş[4], Mostafa Rashdan[5] & Mohammad Salman[5]

Accurate parameter identification in chaotic dynamical systems constitutes a challenging inverse problem due to extreme sensitivity to initial conditions, pronounced nonlinearity, and highly multimodal error landscapes. To address these challenges, this study proposes a global-best-guided electric eel foraging optimization algorithm (g-EEFO), which enhances the original EEFO framework by embedding a behavior-aware and phase-dependent global learning mechanism. Unlike existing EEFO variants that rely solely on stochastic foraging dynamics, g-EEFO integrates global-best information as a soft cooperative signal that modulates the interacting, resting, hunting, and migrating behaviors without overriding them. In this way, global guidance acts as a directional bias rather than a dominant attractor, preserving ecological diversity while strengthening convergence coherence. For the first time, EEFO and its improved variant are applied to chaotic system parameter estimation. The proposed method is evaluated on two representative models: the classical Lorenz system and a structurally richer memristive chaotic system. Extensive numerical experiments, including statistical analysis, convergence profiling, boxplot distributions, and parameter-evolution trajectories, demonstrate the clear superiority of g-EEFO over several state-of-the-art metaheuristics. For the Lorenz system, g-EEFO achieves a best mean squared error of 7.02×10^{-26}, which is six to twenty orders of magnitude lower than competing methods, while maintaining an exceptionally small standard deviation (4.58×10^{-20}). For the memristive system, g-EEFO attains a best error of 8.19×10^{-19}, again outperforming all benchmarks by several orders of magnitude and exhibiting the highest run-to-run stability. In both cases, the estimated parameters match the true system values with near-perfect precision. These results confirm that the proposed behavior-aware global guidance fundamentally reshapes the search dynamics of EEFO, yielding substantial gains in convergence stability, numerical accuracy, and robustness. The g-EEFO therefore provides a powerful and reliable alternative for chaotic parameter identification and nonlinear system reconstruction across diverse dynamical regimes.

Keywords Chaotic systems, Parameter identification, Global-best-guided electric eel foraging optimization algorithm, Parameter identification, Metaheuristics

Chaotic systems occupy a unique position in nonlinear science, as they combine deterministic structure with unpredictable behavior. Their extreme sensitivity to initial conditions, fractal attractors, and long-term divergence make them powerful models for natural and engineered processes, but also render their inverse problems exceptionally difficult. In particular, parameter identification in chaotic dynamics poses a dual challenge: the objective landscape is highly multimodal and irregular, while even minute estimation errors can lead to dramatically different trajectories. Classical analytical and gradient-based techniques are therefore ill-suited to this task. Over the past two decades, population-based metaheuristic optimization has emerged as the most practical and effective paradigm for chaotic system identification, offering robustness against nonconvexity and independence from explicit derivative information. However, the growing complexity of chaotic models and

[1]Department of Electrical and Electronic Engineering, Bursa Uludag University, Bursa 16059, Turkey. [2]Applied Science Research Center, Applied Science Private University, Amman 11931, Jordan. [3]Department of Computer Engineering, Bitlis Eren University, Bitlis 13100, Turkey. [4]Department of Computer Engineering, Istanbul Gedik University, İstanbul, Turkey. [5]College of Engineering and Technology, American University of the Middle East, Egaila 54200, Kuwait. ✉email: davutizci@gmail.com; davutizci@uludag.edu.tr

the demand for higher numerical precision have exposed persistent weaknesses in existing optimizers, such as premature convergence, instability across repeated runs, and loss of accuracy in strongly chaotic regimes. These challenges motivate the search for structurally stronger optimization frameworks that can preserve diversity while achieving coherent and reliable convergence which is an objective that underpins the present study.

Literature review

Chaotic dynamical systems are characterized by strong nonlinearity and extreme sensitivity to initial conditions. These features generate complex attractor geometries and make parameter estimation a demanding inverse problem in nonlinear dynamics. Accurate identification of system parameters is essential in a variety of applications, including secure communications, chaotic encryption, nonlinear circuit modeling, biological system analysis, and advanced control. However, the task remains challenging because the identification landscape is typically multimodal, highly irregular, and rarely admits simple analytical relationships between parameters and observed behavior[1,2]. For these reasons, metaheuristic optimization algorithms have become a widely adopted solution strategy for chaotic parameter estimation over the past two decades.

Beyond their theoretical relevance, metaheuristic optimizers have also become indispensable in practical engineering and applied-science applications[3–9]. They are routinely employed in power system operation, renewable energy management, robotics, controller tuning, biomedical signal processing, structural design, wireless sensor network deployment, and intelligent transportation. Their main advantage is the ability to handle nonconvex and multimodal problems without gradient information—an important feature in real-world scenarios where models may be incomplete, noisy, or strongly nonlinear. In the specific context of chaotic and nonlinear dynamical systems, optimization methods play a central role in system identification, model reconstruction, and predictive control, enabling tasks such as secure data transmission, fault diagnosis, neuromorphic circuit design, and adaptive control of complex processes. As these domains continue to grow, the demand for optimizers that are both numerically precise and consistently robust has become increasingly pronounced.

Early research on chaotic parameter estimation focused largely on improving classical swarm-based methods. Enhanced particle swarm optimization (PSO) schemes[1] and hybrid approaches combining Nelder–Mead simplex search with differential evolution (DE)[2] demonstrated that population-based search can successfully recover chaotic parameters under strong nonlinearity. Building on these foundations, several biologically inspired algorithms were introduced to strengthen global search and reduce susceptibility to local traps. Representative examples include chaotic invasive weed optimization[10], chaotic gravitational search algorithms[11], and oppositional seeker optimization[12]. Additional work proposed hybrid swarm intelligence approaches tailored to canonical benchmarks such as the Lorenz system[13], along with improved forms of teaching–learning-based optimization (TLBO)[14].

A second direction emphasized hybridization, chaos-enhanced operators, and fractional-order formulations to improve exploration and estimation fidelity. Fractional-calculus variants of the firefly algorithm[15], adaptive differential evolution strategies for uncertain nonlinear systems[16], and artificial bee colony methods combined with cuckoo search mechanisms[17] are notable examples. Other studies incorporated cellular structures, sinusoidal search components, and marine-predator-inspired movement patterns. A representative hybrid design combined whale optimization with sine–cosine search and was applied to chaotic systems as well as semiconductor diode models[18]. While such methods often improve exploration capability, their behavior can remain sensitive to landscape irregularities and may still exhibit instability in highly chaotic regimes.

In parallel, evolutionary techniques were developed for fractional-order chaotic dynamics and related identification tasks. Examples include evolutionary approaches for fractional-order chaotic behavior optimization[19], quantum fruit fly optimization for three-dimensional chaotic equations[20], and memory-based PSO variants aimed at improving run-to-run stability[21]. A broader range of metaheuristics has also been explored for fractional-order system identification[22]. More recently, attention has shifted toward data-driven and machine-learning-assisted frameworks, including neural-network-aided parameter estimation and hybrid physics-informed modeling strategies[23,24]. Additional studies have reported the application of aquila optimization to fractional-order chaotic oscillators[25], adaptations of grey wolf optimization for chaotic systems[26], identification of megastable systems with hidden attractors using sparrow search[27], discrete fractional chaotic modeling supported by deep learning[28], and evolutionary swarm approaches tailored to fractional-order dynamics[29]. The increasing adoption of machine learning for nonlinear parameter estimation is further evidenced in recent work[30]. In this study, machine learning is viewed as a complementary future direction—particularly as a surrogate-assisted evaluator—rather than as a replacement for model-based identification.

Alongside these developments, electric eel foraging optimization (EEFO) has gained increasing attention as a flexible and effective metaheuristic for complex engineering problems[31]. The literature reports successful applications of EEFO in diverse domains, such as electric vehicle design optimization[32], hybrid renewable energy systems[33], quantum LSTM training for engineering tasks[34], microgrid controller design[35], microbial fuel cell optimization[36], automotive engine speed regulation[37], and medical image segmentation using dynamic EEFO variants[38]. Collectively, these studies suggest that EEFO offers a strong balance between exploratory diversity and exploitation refinement when solving difficult nonlinear optimization problems.

Despite the breadth of work on chaotic parameter estimation[39–43], the literature reveals a clear gap: EEFO has not previously been employed for chaotic parameter identification, nor has a global-best-guided enhancement of EEFO been developed and validated in this context. This gap is particularly relevant because many existing metaheuristics continue to exhibit premature convergence, reduced precision, or inconsistent behavior across repeated runs when the objective surface is highly chaotic and multimodal. In addition, recent critiques in the optimization community have emphasized that metaphor-driven algorithms can suffer from structural redundancy and benchmarking pitfalls, reinforcing the importance of mechanism-level contributions grounded

in search dynamics rather than narrative novelty. Motivated by this perspective, the present work focuses on a structurally meaningful enhancement—embedding global learning into EEFO in a behavior-aware manner—rather than proposing a purely metaphor-based variant.

Regarding benchmark selection, the literature employs a wide range of chaotic models, including Lorenz, Chen, Lü, Rössler, Chua, and Hindmarsh–Rose systems. Among these, the Lorenz system remains the most commonly used reference for parameter estimation because of its well-known chaotic behavior and extensive prior study. By contrast, memristive chaotic systems are far less explored in identification studies, despite their importance in nonlinear circuit design, neuromorphic computing, and next-generation electronic devices. Memristive dynamics introduce state-dependent current–voltage interactions and memory effects, which typically produce more irregular and demanding error landscapes. Consequently, evaluating performance on both a canonical benchmark (Lorenz) and a structurally richer memristive model provides a meaningful assessment across different levels of dynamical complexity.

Overall, the reviewed literature reflects a clear progression in algorithmic development for chaotic parameter estimation. Early swarm-based and hybrid methods established feasibility but often suffered from instability and premature convergence. Later generations introduced fractional-order modeling, chaos-enhanced operators, and hybrid evolutionary mechanisms to strengthen global search and improve numerical precision. More recent contributions focus on adaptive control of exploration–exploitation balance and richer population dynamics. Nevertheless, many methods still degrade in highly chaotic and multimodal landscapes, particularly in terms of run-to-run stability and high-precision convergence. These persistent limitations motivate the present study, which aims to achieve more coherent global learning while preserving diversity through a behavior-aware, energy-regulated integration strategy within the EEFO framework.

Research motivation

The primary motivation of this work stems from the absence of EEFO-based approaches for chaotic parameter estimation and from the persistent limitations observed in existing metaheuristic methods when confronted with strongly nonlinear and chaotic landscapes. Although numerous optimizers have been proposed for parameter identification, many of them exhibit degraded performance in the presence of extreme sensitivity, multimodality, and fractal-like error surfaces. In such environments, premature convergence, instability across independent runs, and loss of numerical precision are frequently reported. These shortcomings highlight the need for an optimization framework that can preserve exploration in early stages, maintain diversity under severe nonlinearity, and still achieve coherent and accurate convergence.

The selection of EEFO as the foundation of this study is driven by its distinctive behavioral architecture and its demonstrated effectiveness in solving complex engineering problems. Unlike conventional swarm-based algorithms that rely on uniform social learning rules, EEFO is structured around a multi-phase foraging ecology consisting of interacting, resting, hunting, and migrating behaviors. Each phase embodies a different search modality, enabling the population to traverse the search space through heterogeneous movement patterns before progressively refining promising regions. This design is particularly well suited for chaotic parameter estimation, where the objective landscape is highly multimodal and sensitive to small perturbations. In such settings, classical optimizers often fail due to early loss of diversity. By contrast, EEFO's phase-based dynamics inherently sustain population diversity while still enabling effective exploitation in later stages. Recent applications of EEFO in domains such as microgrid control, electric vehicle design, biomedical imaging, and nonlinear control further demonstrate its robustness, adaptability, and scalability under severe nonlinearity, making it a compelling candidate for chaotic system identification.

Building upon these strengths, the present study introduces an enhanced variant, termed g-EEFO. The proposed framework incorporates a behavior-aware global learning mechanism that guides the population toward promising regions without overriding the ecological dynamics of EEFO. The objective is not merely to accelerate convergence, but to reshape the search process so that precision is improved, run-to-run variability is reduced, and robustness is maintained even when the underlying system exhibits extreme chaotic behavior. In this way, g-EEFO addresses the core weaknesses of existing metaheuristics (namely instability and premature convergence) while preserving the exploratory richness that is essential in chaotic landscapes.

To assess the robustness and generality of the proposed method, g-EEFO is evaluated on two distinct chaotic systems. The classical Lorenz system is employed as a canonical benchmark, enabling direct comparison with a large body of existing studies and ensuring methodological transparency. In contrast, a memristive chaotic system is selected to represent a structurally richer and far less explored class of nonlinear dynamics, characterized by state-dependent current–voltage interactions and memory effects. Such systems produce highly irregular error landscapes and pose substantially more demanding identification challenges. By combining these two models, the experimental design spans both a well-established low-dimensional benchmark and a more intricate nonlinear system, allowing the proposed framework to be examined under markedly different dynamical regimes.

Although the present study focuses on two representative systems, the formulation of g-EEFO is independent of the governing equations and dimensionality of the underlying model. The algorithm operates solely on the objective function constructed from observed trajectories and therefore extends naturally to other chaotic and hyperchaotic systems. All behavioral operators and the post-behavioral global guidance act on vector-valued positions without assuming any fixed dimensionality. As problem dimension increases, the principal impact is a proportional rise in computational cost, which is inherent to all population-based metaheuristics. Importantly, the proposed global-best integration does not introduce any dimension-dependent control parameters. The consistent improvements observed across both the canonical Lorenz model and the structurally richer memristive system indicate that the proposed framework enhances robustness and convergence in a model-agnostic manner. Consequently, the reported results are expected to generalize to a broad class of chaotic and

hyperchaotic identification problems, with scalability governed primarily by computational resources rather than by structural limitations of the algorithm.

Novelty and contributions

This study contributes to the field of metaheuristic optimization by introducing a structurally novel mechanism for embedding global learning into a multi-phase ecological optimizer and by demonstrating its effectiveness on one of the most challenging classes of inverse problems; namely chaotic system parameter identification. Rather than proposing yet another metaphor-driven variant, the work advances the design philosophy of population-based optimization by redefining how global knowledge can be integrated without destroying behavioral diversity. The principal contributions of this work are summarized as follows:

1. This work proposes the g-EEFO, in which global information is embedded as a post-behavioral, energy-regulated modulation rather than as a dominant attractor. Unlike conventional gbest-driven schemes, the proposed mechanism preserves the interacting, resting, hunting, and migrating dynamics of EEFO and injects global guidance in a soft, phase-dependent manner. This establishes a new paradigm for integrating global learning into multi-phase bio-inspired optimizers while maintaining diversity and ecological identity. To the best of our knowledge, this is the first framework of its kind.
2. The proposed g-EEFO is applied, for the first time, to the identification of parameters in chaotic dynamical systems. Chaotic landscapes are characterized by extreme sensitivity, strong nonlinearity, and highly multimodal error surfaces, making them stringent testbeds for optimization algorithms. The study demonstrates that the proposed structural enhancement enables EEFO to operate reliably and with unprecedented numerical precision in such environments.
3. The effectiveness of g-EEFO is examined on two representative systems: the canonical Lorenz model and a structurally richer memristive chaotic system. These models span different levels of dynamical and topological complexity, allowing the proposed framework to be assessed under markedly different nonlinear behaviors. This dual-system design provides a meaningful and nontrivial validation of robustness and generality.
4. The study adopts a rigorous multi-level evaluation protocol, including convergence curves, boxplot distributions, parameter-evolution trajectories, residual analyses, and best/mean/worst statistical indicators over multiple independent runs. All competing algorithms operate under identical computational budgets. This exhaustive analysis framework enables a transparent assessment of accuracy, repeatability, and numerical stability.
5. Benchmarking results show that g-EEFO consistently achieves substantially lower objective values and mean squared errors than EEFO and several recent optimizers, including AOO[44], DOA[45], MO[46], and WO[47]. The gains extend beyond final accuracy to convergence speed and run-to-run stability, with improvements reaching multiple orders of magnitude in both test systems. These outcomes confirm that the proposed framework is not an incremental variant but a structurally stronger optimizer for highly complex landscapes.

Collectively, these contributions establish g-EEFO as a methodologically novel and practically powerful optimization framework. Beyond its immediate application to chaotic systems, the proposed behavior-aware global learning strategy provides a transferable blueprint for enhancing a broad class of ecological and multi-phase metaheuristics.

Problem definition

In general, when no prior knowledge of the chaotic system is available, system identification becomes a challenging task, often requiring the selection of system parameters through trial-and-error procedures. As a result, the system identification problem is typically reformulated as a parameter estimation task. Considering a n-dimensional chaotic system defined as follows:

$$\dot{X} = F(X, X_0, \theta) \tag{1}$$

where, $X = (x_1, x_2, \ldots, x_n)^T \in R^n$ is the state vector, $\theta = (\theta_1, \theta_2, \ldots, \theta_m)^T \in R^m$ system parameter vector, X_0 is the initial state of system. $F: R^n \times R^m \to R^n$ is a given non-linear vector function. Given that the structure of the system is known, the identified model can be represented as shown in Eq. (2).

$$\dot{Y} = F(Y, X_0, \widehat{\theta}) \tag{2}$$

where, $Y = (y_1, y_2, \ldots, y_n)^T \in R^n$ is the state vector of the identified system. $\widehat{\theta} = (\widehat{\theta}_1, \widehat{\theta}_2, \ldots, \widehat{\theta}_m)^T \in R^m$ is the identified system parameter. We can represent the problem of parameter identification through Eq. (3).

$$\widehat{\theta} = \arg\min_{\theta} J(\theta) = \arg\min_{\theta} \frac{1}{D_n} \sum_{i=1}^{D_n} \|x_i - y_i\|^2 \tag{3}$$

Here, D_n represents the data length corresponding to the state variables, and x_i and y_i denote the true and estimated values of the system for each state variable, respectively. Based on this analysis, the parameter identification problem of a chaotic system can be reformulated as a multivariable optimization problem in

which the relevant parameters are adjusted to minimize the objective function J[48]. The fundamental concept of parameter estimation for chaotic systems is depicted in Fig. 1.

EEFO and proposed g-EEFO algorithms

Overview of electric eel foraging optimization

Inspiration

The EEFO algorithm, proposed by Zhao et al.[31], incorporates four primary behavioral strategies: interacting, resting, hunting, and migrating. Each of these strategies is mathematically formulated to balance the dual objectives of exploration and exploitation throughout the optimization process. The subsequent subsections present the detailed mathematical formulations corresponding to these mechanisms.

Phase 1: interacting

The interaction behavior among electric eels within a population is defined by two fundamental components. First, an individual eel can establish communication with a randomly selected member of the population, utilizing the positional information of all individuals. During this process, the position update is governed by the difference between the selected eel and the population's central position. Subsequently, the eel may also interact with other randomly chosen individuals, incorporating information gathered from the broader search space. In this phase, the position adjustment is influenced by the deviation between a randomly selected eel and another randomly generated individual within the search domain. This interaction mechanism reflects a stochastic movement in various directions, denoted by C, and can be mathematically modeled as presented in Eq. (4).

$$\begin{cases} \begin{cases} v_i(t+1) = x_j(t) + C \times \left(\bar{x}(t) - x_i(t)\right), & p_1 > 0.5 \\ v_i(t+1) = x_j(t) + C \times \left(x_r(t) - x_i(t)\right), & p_1 \le 0.5 \end{cases} & fit(x_j(t)) < fit(x_i(t)) \\ \begin{cases} v_i(t+1) = x_i(t) + C \times \left(\bar{x}(t) - x_j(t)\right), & p_2 > 0.5 \\ v_i(t+1) = x_i(t) + C \times \left(x_r(t) - x_i(t)\right), & p_2 \le 0.5 \end{cases} & fit(x_j(t)) \ge fit(x_i(t)) \end{cases} \tag{4}$$

Here, p_1 and p_2 denote random numbers uniformly distributed within the interval [0,1]. The term $fit(x_j(t))$ represents the fitness value associated with the i^{th} electic reel at iteration *t*. The variable x_j corresponds to a randomly selected eel from the population *X*, where $j \neq i$. Additionlly, $\bar{x}(t)$ and x_r are determined according to Eq. (5) an Eq. (6), respectively[34].

$$\bar{x}(t) = \frac{1}{n} \sum {}^{n}_{i=0} x_i(t) \tag{5}$$

$$x_r = l + r \times (u - l) \tag{6}$$

Where n denotes the population size, r represents a random vector with elements uniformly distributed in the interval [0,1], and l and u correspond to the lower and upper boundary limits of the search space, respectively.

Phase 2: resting

In the EEFO algorithm, defining a resting area (RA) for electric eels prior to the activation of their resting behavior is a crucial step to enhance search efficiency. The RA is established within the region where one

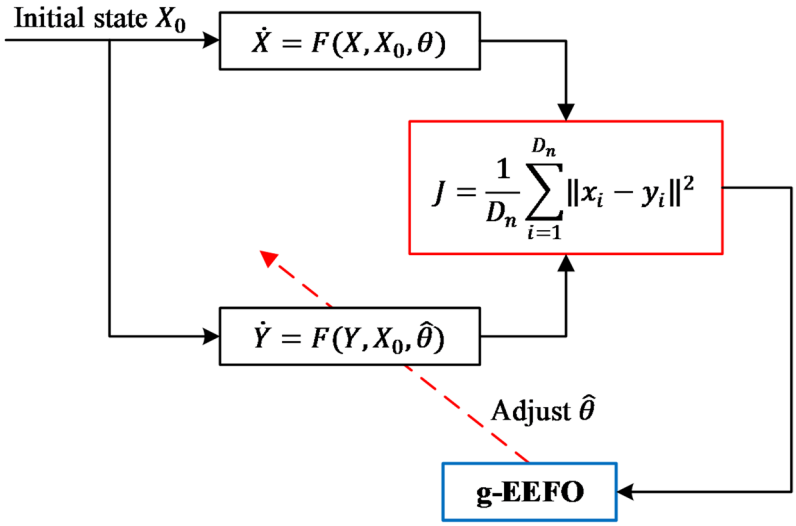

Fig. 1. Schematic representation of the parameter estimation methodology for chaotic systems.

dimension of the eel's value corresponds to the main diagonal of the normalized search space. Subsequently, the eel's values are normalized, and the center of the RA is determined by projecting a randomly selected eel value onto the main diagonal of the normalized domain. After this process, the resting value of the eel is assigned within its corresponding RA before initiating the actual resting behavior.

$$R_i\,(t+1) = Z\,(t) + a \times \left|Z\,(t) - X_b\,(t)\right| \tag{7}$$

$$a = a_0 \times \sin\left(2\pi\, r_2\right) \tag{8}$$

where $X_b\,(t)$ is the positon vector of the best solution, $Z\,(t)$ is computed using the expression $Z\,(t) = z\,(t) \times (u - l) + l$. The scale factor of RA, denoted by a_0, regulates the contraction of the RA range as the iterations progress, and its value is determined according to Eq. (8). Once the RA has been established, the electric eels migrate toward this region to perform their resting behavior. In essence, each eel updates its position by moving toward the RA, thereby aligning with its corresponding resting location within the designated area. This resting mechanism can be formally represented as follows:

$$v_i\,(t+1) = R_i\,(t+1) + n_2 \times \left(R_i(t+1)round(rand) \times x_i(t)\right) \tag{9}$$

Phase 3: hunting

When detecting prey, electric eels display a coordinated swimming behavior, organizing themselves into a broad circular formation around the target rather than engaging in chaotic swarming. Through low-frequency electric organ discharges, they communicate and cooperate effectively. As the interaction progresses, this circular formation gradually contracts, enabling the eels to drive the prey from deeper waters toward shallower areas, thereby making it more vulnerable. The resulting contracted and electrified circle serves as the active hunting zone, causing the prey to move erratically due to fear. The procedure for updating the prey's position within this hunting area, relative to its previous location, is described as follows:

$$H_{prey}\,(t+1) = X_b\,(t) + \beta \times \left|\bar{x}\,(t) - X_b\,(t)\right| \tag{10}$$

$$\beta = \beta_0 \times \sin\left(2\pi\, r_3\right) \tag{11}$$

The parameter ß, computed using Eq. (11), defines the scale of the hunting area, which gradually decreases as iterations progress. Once the hunting zone is established, an electric eel begins the prey-capturing process within this defined region. During the pursuit, the eel swiftly identifies the prey's updated position and coils its body—bringing its head and tail together—to encircle the target. Concurrently, it emits a high-voltage discharge around the entrapped prey. Within the EEFO algorithm, this hunting behavior is modeled through the coiling mechanism, wherein the eel's position dynamically adjusts to align with the prey's updated location. The coiling behavior of electric eels during hunting is mathematically formulated in Eq. (12):

$$v_i\,(t+1) = H_{prey}\,(t+1) + \eta \times \left(H_{prey}\,(t+1) - round(rand) \times x_i(t)\right) \tag{12}$$

where η denotes the coiling (or curling) factor, the value of which is determined according to Eq. (13).

$$\eta = e^{\frac{r_4(1-t)}{T}} \times \cos\left(2\pi\, r_4\right) \tag{13}$$

Phase 4: migrating

Upon identifying potential prey, electric eels transition from their RA toward the predefined hunting region. This migratory behavior of the eels is mathematically formulated and represented using Eq. (14):

$$v_i\,(t+1) = -r_5 \times R_i\,(t+1) + r_6 \times H_r\,(t+1) - L \times \left(H_r\,(t+1) - x_i\,(t)\right) \tag{14}$$

$$H_r\,(t+1) = X_b\,(t) + \beta \times \left|\bar{x}\,(t) - X_b\,(t)\right| \tag{15}$$

In Eq. (14), H_r represents any position within the hunting region, while r_5 and r_6 are random values uniformly distributed between 0 and 1. The term $\left(H_r\,(t+1) - x_i\,(t)\right)$ characterizes the eel's directional movement toward the hunting zone. L denotes the Lévy flight mechanism, which enhances the exploitation phase of the EEFO algorithm by mitigating the risk of premature convergence to local optima.

By emitting low-intensity electric discharges, an eel is capable of sensing the prey's location and dynamically adjusting its position accordingly. During the foraging process, when the eel detects the proximity of prey, it relocates toward the identified position; otherwise, it retains its current location. The mathematical formulation governing the position update of eels is expressed as follows:

$$x_i\,(t+1) = \begin{cases} x_i\,(t), & fit\left(x_i\,(t)\right) \leq fit\left(v_i\,(t+1)\right) \\ v_i\,(t+1), & fit\left(x_i\,(t)\right) > fit\left(v_i\,(t+1)\right) \end{cases} \tag{16}$$

Shifting from exploration to exploitation

The search dynamics of the EEFO algorithm are governed by an energy factor, which strategically regulates the transition between exploration and exploitation to enhance optimization efficiency. This energy factor serves as

a decisive criterion in determining whether the algorithm engages in exploratory or exploitative behavior. The mathematical formulation of the energy factor is defined as follows:

$$E(t) = 4 \times ln\left(\frac{1}{r_7}\right) \times \sin\left(1 - \frac{t}{T}\right) \tag{17}$$

In the aforementioned equation, the energy factor $E(t)$ gradually decreases with the progression of iterations, exhibiting a declining trend accompanied by slight fluctuations. When $E(t) > 1$, the eels engage in extensive exploration across the entire search space through interactive behaviors. Conversely, when $E(t) \leq 1$, the eels focus on exploiting potential regions by performing migration, resting, or hunting activities within a promising subspace. In the early stages of the optimization process, exploration predominates, whereas exploitation becomes more dominant in the later phases[34].

Proposed Gbest operator-based electric eel foraging optimization (g-EEFO)

Figure 2 illustrates the conceptual framework of the proposed g-EEFO algorithm. The method extends the original EEFO by embedding a global learning mechanism that enhances convergence coherence while preserving the ecological dynamics of eel foraging. The algorithm begins with the initialization of control parameters and the random generation of an eel population. The fitness of each individual is then evaluated to quantify its performance in the search space. At each iteration, every eel executes exactly one of the four canonical EEFO behaviors (interacting, resting, hunting, or migrating) according to the control variable E and the associated probabilistic rules. These behaviors collectively regulate the exploration–exploitation process through heterogeneous movement patterns. Once the behavior-specific position update is completed, the gbest operator is invoked as a post-behavioral refinement step. In other words, the position produced by the selected EEFO behavior is softly adjusted using the gbest guidance rule before proceeding to the next iteration. The block labeled "Execute gbest method" in Fig. 2 therefore corresponds to a modulation stage applied after interacting, resting, hunting, or migrating and before incrementing the iteration counter. The process repeats until the termination condition (maximum number of iterations) is met, at which point the best solution found so far is returned.

The gbest operator is inspired by the social learning principle of PSO, where each agent's motion is influenced by both its own experience and the globally best solution discovered by the population. The choice of a PSO-style gbest mechanism is deliberate. It provides a compact and lightweight representation of collective learning, conveying global information through a simple directional cue rather than through heavy-handed attraction.

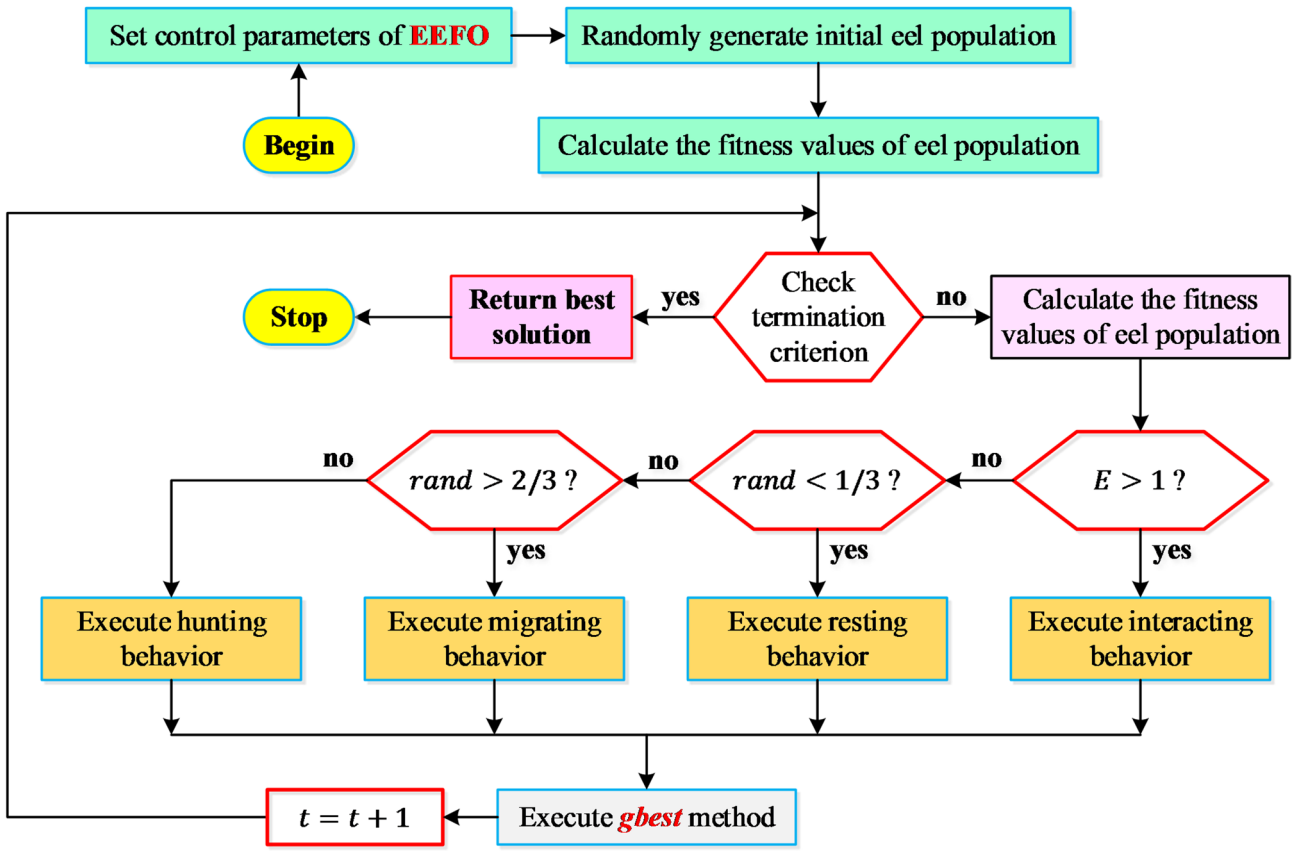

Fig. 2. Conceptual framework of proposed g-EEFO.

This property is conceptually compatible with eel foraging behavior, where individuals do not abandon their intrinsic motion patterns but subtly adjust their trajectories in response to weak global cues, such as electric field disturbances or collective sensing of prey movement. In natural eel swarms, coordinated hunting emerges from local actions modulated by shared environmental signals rather than from rigid leader-following. Analogously, in g-EEFO, the gbest term does not impose a deterministic pull; it introduces a soft directional tendency that complements the interacting, resting, hunting, and migrating behaviors. This design preserves ecological diversity while enabling coherent population-level learning.

Mathematically, the position of the i^{th} agent is denoted by x_i, and the objective function by $f(x)$. At each iteration, a PSO-inspired auxiliary velocity is computed as[49]:

$$v_i(t+1) = w \cdot v_i(t) + c_1 \cdot rand_1 \cdot (Pbest_i - x_i(t)) + c_2 \cdot rand_2 \cdot (Gbest - x_i(t)) \tag{18}$$

where w is the inertia weight, c_1 and c_2 are acceleration coefficients, and $rand_1, rand_2 \in [0,1]$. The corresponding position update is given as follows.

$$x_i(t+1) = x_i(t) + v_i(t+1) \tag{19}$$

In g-EEFO, this velocity is not maintained as a persistent state variable. It is computed only transiently to generate a directional correction after the EEFO behavioral update and is discarded thereafter. Thus, g-EEFO does not evolve velocity memory as in PSO; the long-term dynamics remain governed by the EEFO ecological phases. The termination of g-EEFO is governed solely by a fixed maximum number of iterations T. No auxiliary convergence thresholds or stagnation tests are employed. All algorithms therefore evolve under identical computational budgets, ensuring fair comparison. When $t = T$, the best solution obtained is returned.

The novelty of g-EEFO does not lie in merely adopting a global-best concept (well established in swarm intelligence) but in how this concept is embedded into the ecological structure of EEFO. In classical gbest-driven algorithms, agents are continuously and uniformly attracted toward the global best, often leading to rapid convergence at the expense of diversity. In contrast, g-EEFO preserves the four-phase foraging dynamics of electric eels and introduces global information as a behavior-aware, post-action bias. The gbest term does not override interacting, resting, hunting, or migrating; it gently realigns the outcome of a biologically inspired action toward globally promising regions. Because this bias is applied only after a behavioral move, the stochastic and ecological nature of EEFO is preserved while the search trajectory gains coherent direction.

A well-known drawback of strong global-best attraction is premature convergence, particularly in multimodal and chaotic landscapes. g-EEFO explicitly avoids this failure mode through three mechanisms: (i) the gbest term is applied only as a transient post-behavioral modulation, not as a persistent driving force; (ii) its influence is regulated by the energy factor, remaining weak during early exploration and strengthening only during exploitation; and (iii) intrinsic EEFO behaviors remain the primary drivers of motion. As a result, diversity is preserved, multiple regions continue to be sampled, and the population avoids early collapse into suboptimal basins.

From a search-dynamics perspective, the gbest strategy introduces an additional, orthogonal control channel. In the original EEFO, exploration–exploitation balance is governed solely by the energy factor, which switches the population between wide-ranging stochastic motion and localized refinement. While effective, this mechanism relies entirely on random ecological movement to achieve global alignment. In g-EEFO, post-behavioral gbest modulation adds a low-dimensional global signal. During early iterations, when E enforces exploration, this signal remains weak and the population continues broad sampling through interacting and migrating. As E decreases, the gbest influence grows, compressing the search around high-quality basins. This two-layer regulation—ecological phase control combined with energy-regulated global guidance—produces a smoother transition between exploration and exploitation, reduces random drift in later stages, and shortens the expected path to the optimum. These mechanisms explain the observed gains in convergence speed, numerical precision, and run-to-run stability, particularly in highly multimodal and chaotic landscapes.

Selected chaotic systems

It is important to note that the present study does not employ any external or empirical datasets. All experiments are conducted using model-generated time-series derived directly from the governing equations of the considered chaotic systems. For each system, a reference trajectory is first produced by numerically integrating the true model with known parameter values and fixed initial conditions. These trajectories serve as synthetic observation data. The parameter identification task is then formulated as the minimization of the discrepancy between the reference trajectory and the trajectory reconstructed using candidate parameter vectors. In all experiments, numerical integration is performed over the same time horizon and with identical step sizes for both the reference and reconstructed systems, ensuring strict comparability. Each metaheuristic algorithm operates under identical population sizes, iteration limits, and initial conditions, and all simulations are repeated for 20 independent runs to evaluate robustness and statistical stability.

Test system 1: Lorenz chaotic system

The Lorenz system, first introduced by Edward N. Lorenz[50] in 1963, is one of the most well-known examples of deterministic chaos in nonlinear dynamical systems[13,21]. Originally developed to model atmospheric convection, the Lorenz system is governed by a set of three coupled, first-order nonlinear differential equations that describe the time evolution of the state variables x_1, x_2 and x_3. In this system, a_1 denotes the Prandtl number, a_2 represents the ratio of the Rayleigh number to the critical Rayleigh number $\left(b = \frac{R_a}{R_c}\right)$, and a_3 characterizes

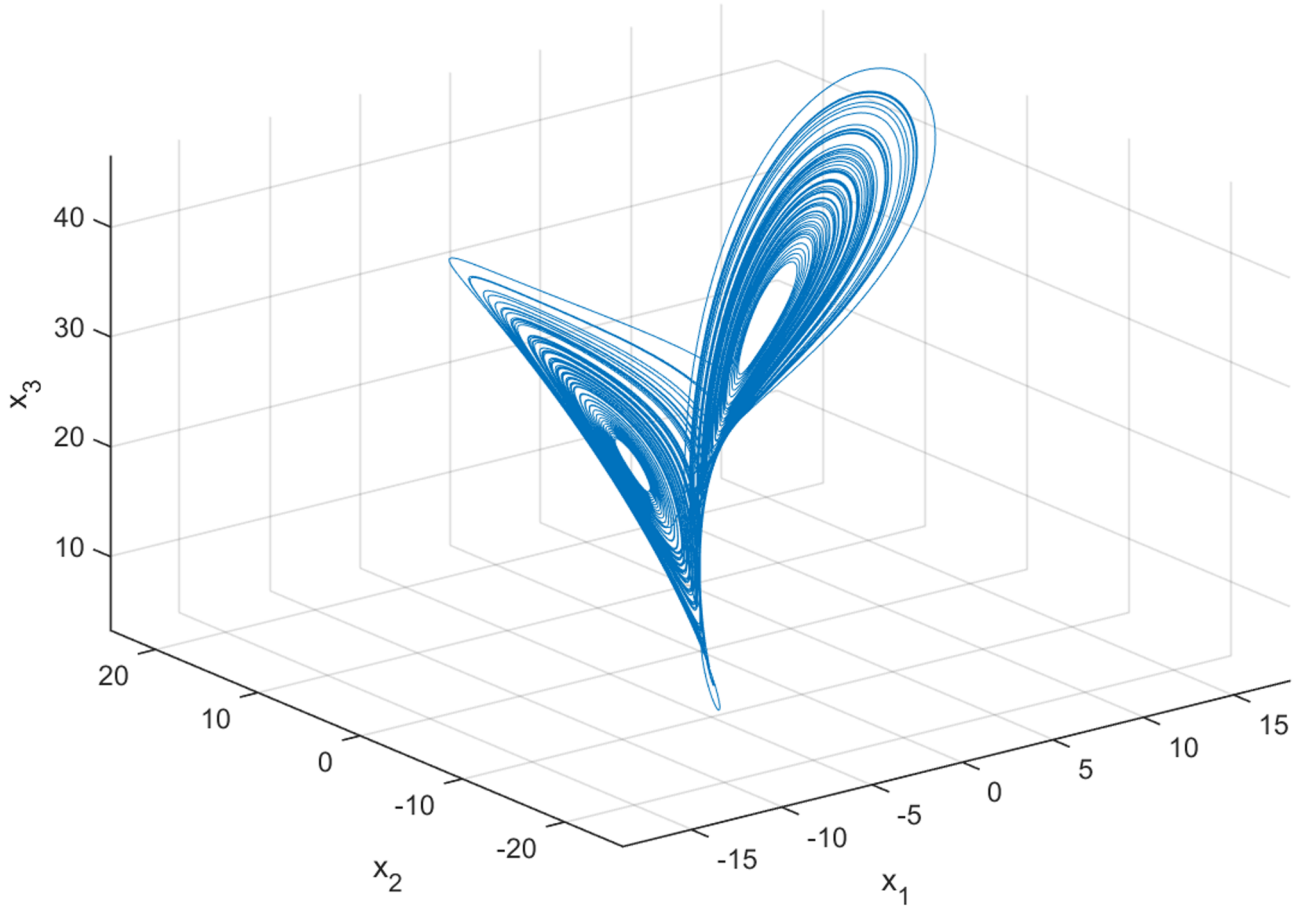

Fig. 3. Three-dimensional phase trajectory of the Lorenz system.

Model equations	Parameter range	Actual model parameters	Initial states
$\frac{dx_1}{dt} = a_1(x_2 - x_1)$ $\frac{dx_2}{dt} = a_2 x_1 - x_1 x_3 - x_2$ $\frac{dx_3}{dt} = x_1 x_2 - a_3 x_3$	$0 \leq a_1 \leq 20$ $0 \leq a_2 \leq 50$ $0 \leq a_3 \leq 5$	$a_1 = 10$ $a_2 = 28$ $a_3 = 8/3$	$x_1(0) = 0.1$ $x_2(0) = 0.1$ $x_3(0) = 0$

Table 1. Details of Lorenz chaotic system.

the geometric scale of the region described by the model. All parameters are assumed to be positive, and the system exhibits a chaotic attractor when $a_1 = 10$, $a_2 = 28$, $a_3 = 8/3$. Moreover, this system displays unstable dynamical behavior, demonstrating sensitivity to initial conditions and containing infinitely many unstable periodic orbits. In this study, the time series generated with parameters $a_1 = 10$, $a_2 = 28$, $a_3 = 8/3$ represent the real case under investigation, and the chaotic behavior of the Lorenz system is illustrated in Fig. 3.

To minimize computational time, the step size h was set to 0.01, and the number of sampling points was defined as $M = 300$. Please note that a_1, a_2 and a_3 estimation is the main goal of this propose. The model equations, parameter ranges, actual model parameters, and initial state values of the Lorenz chaotic system are presented in Table 1.

Test system 2: memristive chaotic system

Chaotic behavior in memristive systems emerges from the intrinsic nonlinearity between the memristor's internal state and its voltage–current characteristics. In general, a memristive system can be represented by a set of nonlinear differential equations that couple the system's state variables with the memristor dynamics. Although memristive chaotic systems have been relatively less explored in the optimization context, they are utilized in this study to enhance the dynamic behavior and solution diversity of the proposed approach. Figure 4 illustrates the simplest model of a memristor-based chaotic circuit, while Table 2 presents a typical mathematical formulation of a memristive chaotic system.

In this study, the time series generated with parameters $a_1 = 1$, $a_2 = 1/3$, $a_3 = 0.6$, $a_4 = 1.5$ represent the real case under investigation, and the chaotic behavior of the memristive system is illustrated in Fig. 5. Please note that a_1, a_2, a_3 and a_4 estimation is the main goal of this propose. To minimize computational

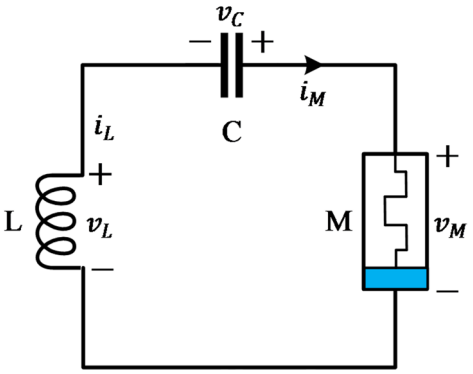

Fig. 4. The simplest memristor-based chaotic circuit model.

Model equations	Parameter range	Actual model parameters	Initial states
$\frac{dx_1}{dt} = a_1 x_2$ $\frac{dx_2}{dt} = -a_2 \left(x_1 + a_4 \left(x_3^2 - 1\right) x_2\right)$ $\frac{dx_3}{dt} = x_2 + x_2 x_3 - a_3 x_3$	$0 \leq a_1 \leq 3$ $0 \leq a_2 \leq 2$ $0 \leq a_3 \leq 3$ $0 \leq a_4 \leq 2$	$a_1 = 1$ $a_2 = 1/3$ $a_3 = 0.6$ $a_4 = 1.5$	$x_1(0) = 0.1$ $x_2(0) = 0$ $x_3(0) = 0$

Table 2. Details of memristive chaotic system.

time, the step size h was set to 0.01, and the number of sampling points was defined as $M = 500$. The model equations, parameter ranges, actual model parameters, and initial state values of the memristive chaotic system are presented in Table 2.

Numerical simulations

Compared algorithms

To evaluate the accuracy and effectiveness of the proposed g-EEFO algorithm, unknown parameters were estimated separately for two distinct chaotic systems: the widely studied Lorenz system, which has been frequently employed in recent research, and the relatively less explored memristive chaotic system. Each of these chaotic systems exhibits unique nonlinear dynamic characteristics. The performance of the proposed g-EEFO was compared with five state-of-the-art metaheuristic algorithms, namely EEFO, AOO, DOA, MO, and WO. The parameter ranges and configuration settings for both systems are summarized in Tables 1 and 2. All algorithms were executed under identical experimental conditions. The complete parameter settings of all algorithms, including population size, iteration limits, and method-specific control coefficients, are summarized in Table 3 to ensure transparency and reproducibility. Each parameter estimation experiment was independently repeated 20 times, and the statistical results were averaged across these runs to ensure reliability. All simulations were carried out using MATLAB R2019a on an Intel Core i7 CPU (2.30 GHz) system equipped with 24 GB of RAM.

The selection of the comparative algorithms is guided by their structural diversity, recency, and demonstrated capability in solving highly nonlinear and multimodal optimization problems. EEFO is included to quantify the direct impact of the proposed global-best enhancement. AOO and DOA represent recent population-based optimizers that emphasize adaptive exploration and exploitation mechanisms, making them suitable references for inverse problems characterized by rugged error surfaces. MO and WO are included as representative metaheuristics with strong global search components and widespread adoption in nonlinear system modeling and parameter estimation studies. Collectively, these algorithms span different design philosophies (ecological, physics-inspired, and behavior-driven search) and therefore provide a balanced and meaningful benchmark set for evaluating performance in chaotic parameter identification tasks, where robustness, precision, and run-to-run stability are critical.

Results of Lorenz chaotic system

The Lorenz benchmark was initially employed to assess the capability of the proposed g-EEFO algorithm in accurately recovering system parameters while maintaining high run-to-run consistency under a standardized experimental setup (20 independent runs, a population size of 30, and 200 iterations). The algorithm's performance was analyzed using multiple diagnostic visualizations and statistical summaries, including a boxplot of objective values, descriptive statistics, convergence trajectories, comparative Mann-Whitney U-test[51], objective function value graphs of 6 algorithms in all runs, parameter evolution curves for a_1, a_2 and a_3 and the final parameter estimates along with their residuals. A comparative analysis with results reported in the literature was also conducted.

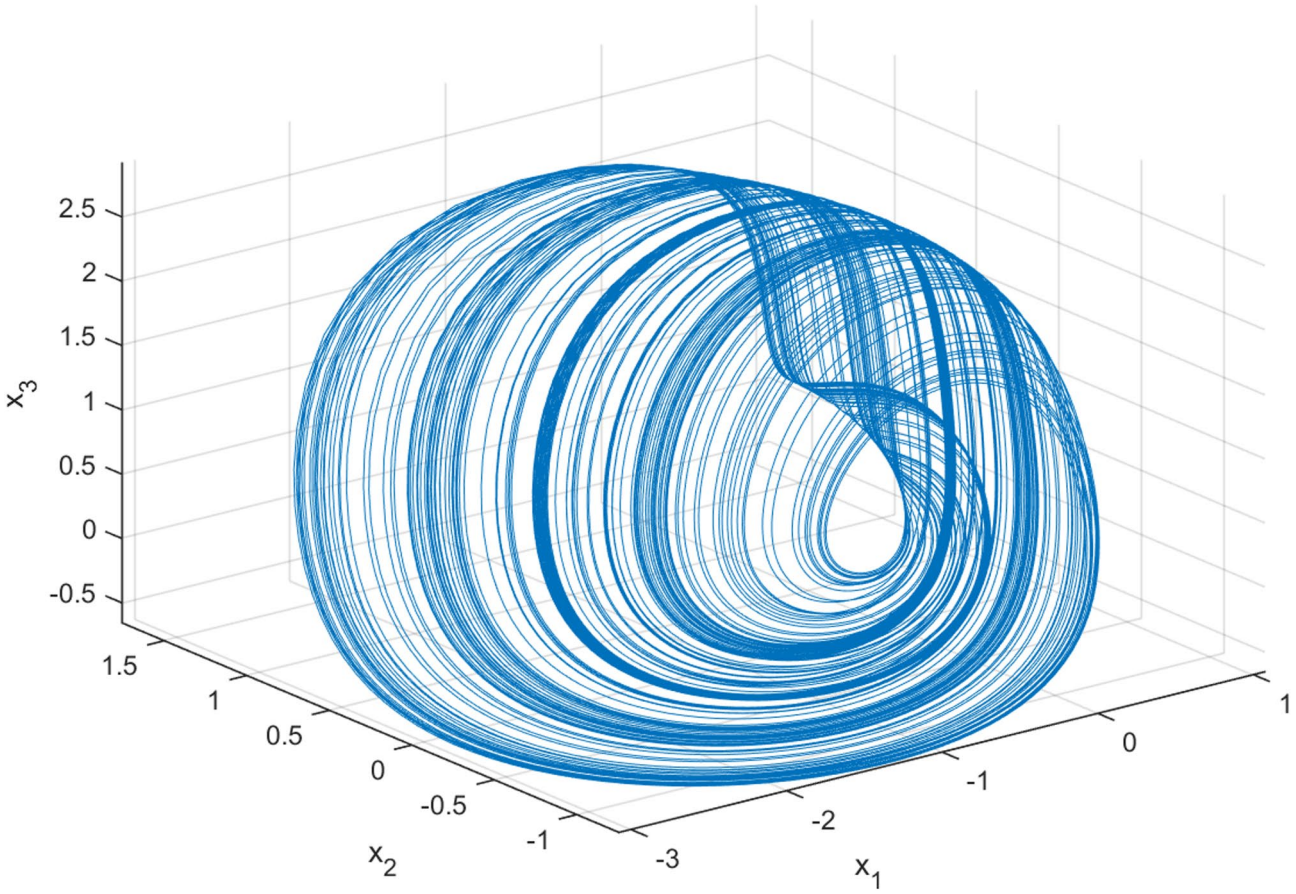

Fig. 5. Three-dimensional phase trajectory of the memristive system.

Figure 6 presents the objective function values of 20 independent runs for six algorithms: the proposed g-EEFO, EEFO, AOO, DOA, MO, and WO, on the Lorenz system parameter identification task. The results demonstrate that the g-EEFO consistently achieves the lowest objective function values across all runs, indicating superior optimization accuracy and convergence reliability. The stability of g-EEFO's performance across iterations suggests that its enhanced global-best learning strategy effectively prevents premature convergence and enhances the algorithm's ability to reach the true global optimum.

In contrast, the competing methods—particularly DOA, MO, and WO—exhibit significantly higher and more fluctuating objective function values, implying weaker search precision and reduced stability. Overall, the g-EEFO not only provides more accurate parameter estimation but also maintains robustness against stochastic variations between runs.

Figure 7 illustrates the comparative boxplots of the objective function values obtained for the Lorenz system using six optimization algorithms: g-EEFO, EEFO, AOO, DOA, MO, and WO. The dispersion and median levels clearly highlight the superior performance of the proposed g-EEFO algorithm. Its boxplot is highly compact, with minimal variance and the lowest median value, indicating consistent convergence toward the global optimum with exceptional accuracy and stability across all independent runs. Conversely, the EEFO algorithm

Algorithm	Population size	Total number of iterations	Other parameters
g-EEFO	30	200	$c_1 = 2,\ c_2 = 2,\ w_{min} = 0.2,\ w_{max} = 0.9$
EEFO	30	200	---
AOO	30	200	---
DOA	30	200	$u = 0.9$
MO	30	200	$G_1 = 0.001,\ G_2 = 100,\ \beta = 0.01$
WO	30	200	$p = 0.4$

Table 3. Parameter settings of algorithms.

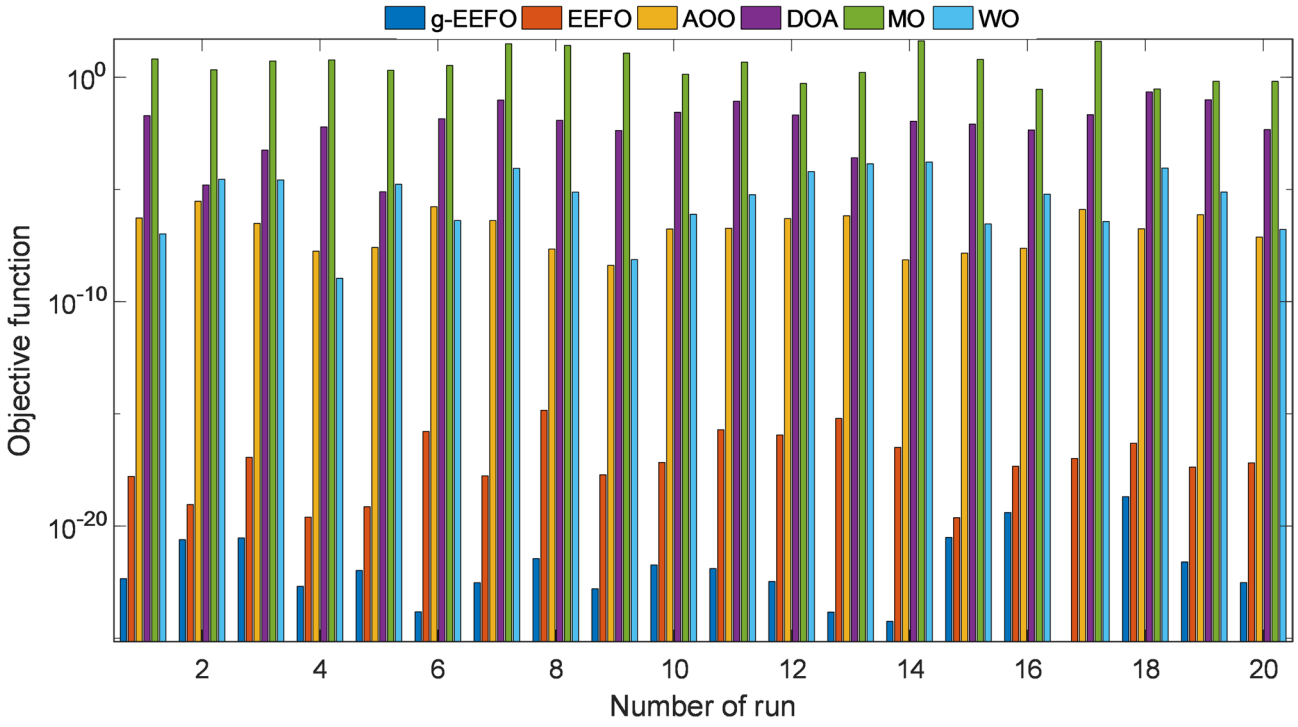

Fig. 6. Objective function values of six algorithms (g-EEFO, EEFO, AOO, DOA, MO, and WO) over 20 independent runs for the Lorenz system.

exhibits a marginally broader solution spread, a phenomenon attributed to the omission of the gbest-guided mechanism, which results in a moderate decline in stability. The remaining algorithms (AOO, DOA, MO, and WO) show significantly larger spreads and higher median values, implying inferior optimization performance and weaker convergence reliability. Among them, MO and DOA demonstrate particularly poor results, as their objective function values remain several orders of magnitude higher.

Table 4 presents the statistical results of the parameter estimation task for the Lorenz system using six optimization algorithms: g-EEFO, EEFO, AOO, DOA, MO, and WO. The metrics reported include the best, worst, average, and standard deviation (SD) of the objective function values obtained from 20 independent runs. As seen in the table, the proposed g-EEFO algorithm achieves the lowest best, worst, and average objective function values, accompanied by the smallest standard deviation (4.5776E − 20). This indicates not only superior optimization accuracy but also remarkable consistency and robustness across multiple runs. In comparison, other algorithms—particularly MO and DOA—exhibit significantly higher average errors and larger standard deviations, reflecting weaker convergence stability. These findings confirm that the introduction of the global best guidance mechanism (gbest) within EEFO significantly enhances its exploration–exploitation balance, leading to more precise and reliable parameter estimation in chaotic system modeling.

Table 5 presents the results of the Mann–Whitney U-test performed to statistically compare the performance of the proposed g-EEFO algorithm with five competing metaheuristic methods on the Lorenz chaotic system. The p-values obtained in all comparisons are significantly lower than the standard significance threshold ($\alpha = 0.05$), confirming that the performance differences between g-EEFO and each benchmark algorithm are statistically significant. Furthermore, the decision variable $h = 1$ in every comparison indicates that the null hypothesis—stating that both algorithms perform equivalently—was rejected in favor of the alternative hypothesis. In all cases, the Winner column identifies g-EEFO as the superior algorithm.

These statistical results strongly reinforce the conclusions drawn from the objective value analysis and boxplot evaluations: g-EEFO achieves not only numerically superior performance but also statistically significant improvements. Thus, the incorporation of the global-best guidance mechanism within the EEFO framework yields a robust and consistently outperforming optimization approach for chaotic system parameter estimation.

Table 6, presents a comparative performance analysis of six distinct optimization algorithms (g-EEFO, EEFO, AOO, DOA, MO, and WO) on the task of parameter estimation (identification) for the chaotic Lorenz system. The performance is evaluated based on the best mean squared error (MSE) achieved and the corresponding estimated values for the system's three parameters (a_1, a_2, a_3). The objective is to achieve the lowest possible MSE, which corresponds to finding the parameter values that most closely match the true parameters of the Lorenz system. Extremely low, logarithmic MSE values signify superior estimation performance. The g-EEFO algorithm registers an exceptionally low MSE value of 7.0213E − 26, which is significantly superior to all other competing algorithms. This result indicates that g-EEFO captures the dynamics of the Lorenz system with an extraordinary level of accuracy. The EEFO algorithm achieves the second-best performance with an MSE of 2.3514E − 20. While higher than g-EEFO, this value is still substantially lower than the remaining four

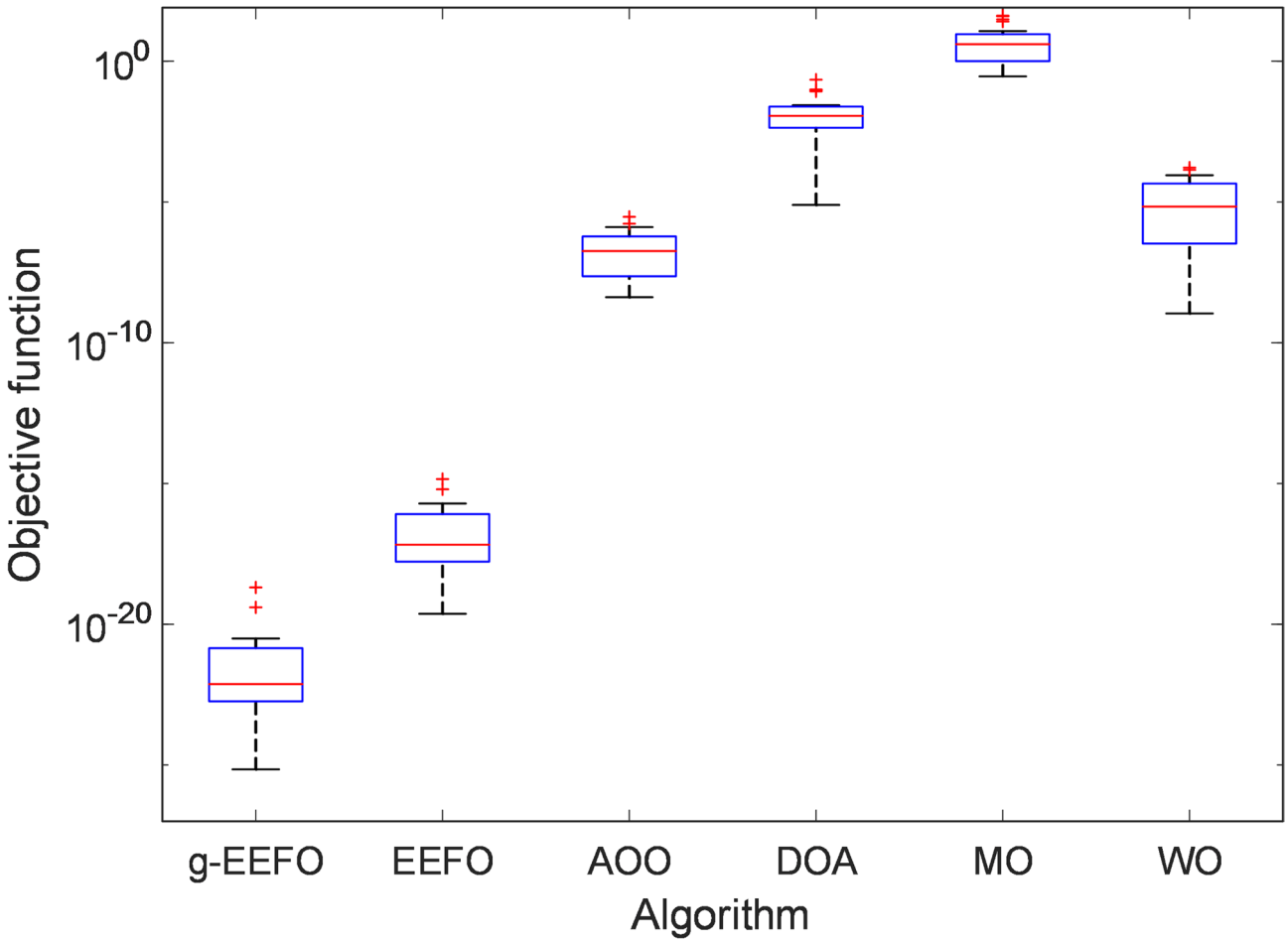

Fig. 7. Comparative boxplots of the objective function values obtained for the Lorenz system.

Algorithm	Best	Worst	Average	SD
g-EEFO	7.0213E−26	2.0347E−19	1.2655E−20	4.5776E−20
EEFO	2.3514E−20	1.4364E−15	1.3322E−16	3.3863E−16
AOO	4.1356E−09	2.9695E−06	4.9181E−07	7.4007E−07
DOA	7.8296E−06	2.2115E−01	3.2742E−02	5.4401E−02
MO	2.9042E−01	4.1611E+01	9.5431E+00	1.3409E+01
WO	1.0992E−09	1.6645E−04	3.2224E−05	5.0021E−05

Table 4. Statistical comparison of optimization algorithms for Lorenz system parameter estimation.

Algorithm	*p*-value	h	Winner
g-EEFO versus EEFO	1.6571E−07	1	g-EEFO
g-EEFO versus AOO	6.7956E−08	1	g-EEFO
g-EEFO versus DOA	6.7956E−08	1	g-EEFO
g-EEFO versus MO	6.7956E−08	1	g-EEFO
g-EEFO versus WO	6.7956E−08	1	g-EEFO

Table 5. Comparative Mann-Whitney U-test results for Lorenz chaotic system.

Algorithm	Best MSE	a_1	a_2	a_3
g-EEFO	7.0213E−26	10.000000000000	28.000000000000	2.666666666667
EEFO	2.3514E−20	9.999999999902	28.000000000069	2.666666666655
AOO	4.1356E−09	10.000039767205	27.999990273977	2.666668285771
DOA	7.8296E−06	9.999690279465	28.001660532305	2.666609718905
MO	2.9042E−01	10.324423786152	27.712390036277	2.711774837202
WO	1.0992E−09	9.999981108539	28.000020109259	2.666664283275

Table 6. Comparative best MSE values and estimated parameters of Lorenz system.

Algorithm	$Error\_rate = \frac{\lvert Actual - Estimation \rvert}{\lvert Actual \rvert} \times 100$		
	a_1	a_2	a_3
g-EEFO	1.0658E−12%	3.4258E−13%	6.9944E−13%
EEFO	9.8000E−10%	2.4643E−10%	4.3750E−10%
AOO	3.9767E−04%	3.4736E−05%	6.0716E−05%
DOA	3.0972E−03%	5.9305E−03%	2.1355E−03%
MO	3.2442%	1.0272%	1.6916%
WO	1.8891E−04%	7.1819E−05%	8.9377E−05%

Table 7. Parameter Estimation error rates of six optimization algorithms for the Lorenz system.

algorithms (AOO, DOA, MO, WO), pointing to a high level of precision. AOO, WO, and DOA exhibit moderate performance, with MSE values ranging from 10^{-9} to 10^{-6}. These algorithms demonstrate errors that are millions of times greater in magnitude compared to the EEFO methods. The MO algorithm records the highest MSE of 2.9042E−01, which is close to 1, indicating the worst performance. This suggests that MO is the least successful algorithm in accurately identifying the Lorenz system parameters. The estimated parameter values reveal not only the algorithms' ability to minimize error but also their precision in locating the correct parameters (The true Lorenz parameters are typically assumed to be $a_1 = 10$, $a_2 = 28$ and $a_3 = 2.666667$). The parameters a_1, a_2 and a_3 estimated by g-EEFO achieve the highest fidelity to the known theoretical values. For example, a_1 and a_2 are perfectly matched to 10.0 and 28.0, while a_3 also shows the highest decimal place accuracy. EEFO also demonstrates very high precision, with a slight decrease in accuracy compared to g-EEFO, consistent with the difference in their MSE values. The MO algorithm, which has the highest MSE, yields parameter estimates that are the furthest from the theoretical values (e.g., $a_1 = 10.3244$, $a_2 = 27.7124$). This indicates that the algorithm not only failed to minimize the error effectively but also converged to physically inaccurate parameter sets.

Table 7 reports the percentage error rates for the estimated parameters a_1, a_2 and a_3 of the Lorenz system using six optimization algorithms. The results clearly show that the proposed g-EEFO achieves extremely low error levels, on the order of 10^{-13}%–10^{-12}%, demonstrating near-perfect parameter identification accuracy. The standard EEFO method also provides strong performance, yet its error rates remain several orders of magnitude higher than those of g-EEFO. Among the competing algorithms, AOO and WO exhibit moderate accuracy with errors ranging between 10^{-5}%–10^{-4}%. In contrast, DOA and especially MO yield the largest deviations from the true parameter values, reaching error rates in the percent range.

The convergence curve analysis presented in Fig. 8 provides definitive insights into the final performance and efficiency of the six optimization algorithms for the Lorenz chaotic system. Observing the descent of the logarithmically scaled MSE objective function on the vertical axis, the g-EEFO algorithm demonstrated the unequivocally superior performance, converging to the lowest value, approximately 10^{-25}, after 200 iterations, which is consistent with the preceding statistical results. The EEFO algorithm performed second best, converging around 10^{-20}, and both EEFO-based methods exhibited a faster and more sustained convergence rate, characterized by a steeper descent compared to the other algorithms. In contrast, AOO, DOA, and MO showed a slow, gradual decrease, stagnating at high objective function values (10^{-10} and above), with MO yielding the worst final result (around 10^{0}). Consequently, the convergence analysis confirms that g-EEFO provides both the highest accuracy and the best optimization efficiency for this challenging parameter identification task.

Figures 9 and 10, and 11, which illustrate the optimization curves for parameters a_1, a_2 and a_3, visually confirm the accuracy and convergence rate of the six algorithms in identifying the Lorenz system. Across all three parameter estimations, the g-EEFO and EEFO algorithms demonstrate the fastest convergence to the true parameter values (hypothetically $a_1 = 10$, $a_2 = 28$, $a_3 \approx 2.667$) following initial transient fluctuations, settling into the closest and most stable results. Notably, g-EEFO exhibits the highest stability and precision in all three plots, settling into a near-horizontal line at or very close to the true value by the 150th iteration or earlier. In sharp contrast, the MO algorithm displays the largest deviation for all three parameters, converging around ≈ 10.3 for a_1, ≈ 27.7 for a_2, and ≈ 2.71 for a_3, which are significantly distant from the target values. The remaining algorithms (AOO, DOA, WO), although eventually converging close to the true value for a_3, either required a longer time to stabilize or displayed slight persistent deviations from the desired true parameters.

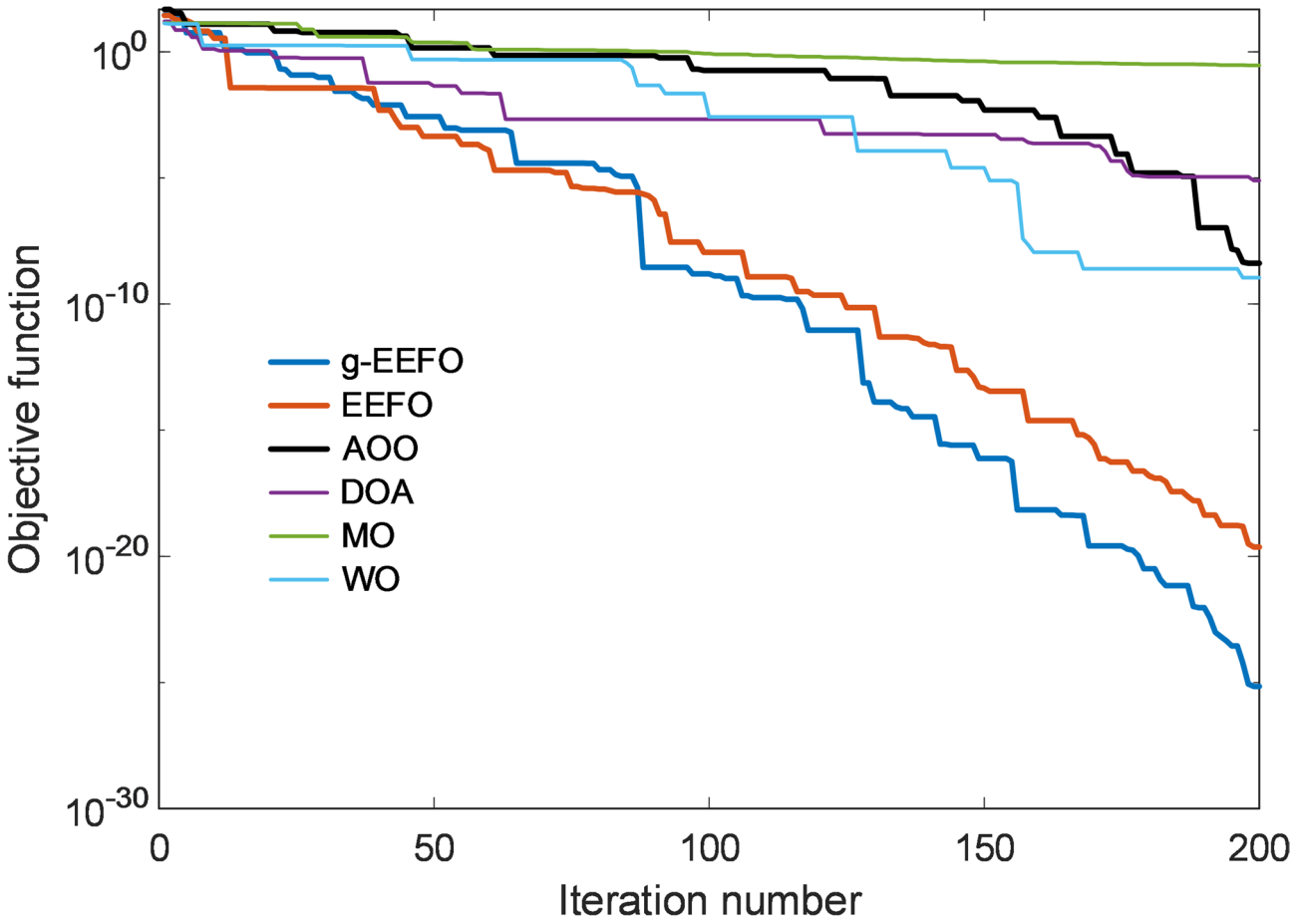

Fig. 8. Convergence curve of MSE objective function for Lorenz chaotic system.

Overall, these curves affirm that g-EEFO not only minimizes the objective function most effectively but also proves unrivaled in parameter estimation by converging to the physically correct parameter values most rapidly and accurately.

Results of memristive chaotic system

The memristive benchmark was initially employed to assess the capability of the proposed g-EEFO algorithm in accurately recovering system parameters while maintaining high run-to-run consistency under a standardized experimental setup (20 independent runs, a population size of 30, and 200 iterations). The algorithm's performance was analyzed using multiple diagnostic visualizations and statistical summaries, including a boxplot of objective values, descriptive statistics, convergence trajectories, comparative Mann-Whitney U-test, objective function value graphs of 6 algorithms in all runs, parameter evolution curves for a_1, a_2, $a_3$and a_4 and the final parameter estimates along with their residuals.

Figure 12 presents the objective function values from 20 independent runs for six algorithms—g-EEFO, EEFO, AOO, DOA, MO, and WO—applied to the memristive system parameter identification problem. The g-EEFO consistently yields the lowest objective function values, demonstrating superior optimization accuracy and stable convergence. Its enhanced global-best learning strategy effectively avoids premature convergence and reliably guides the search toward the true optimum. In comparison, the other algorithms—especially DOA, MO, and WO—produce higher and more variable objective function values, indicating lower estimation precision and reduced robustness across runs.

Figure 13 presents the comparative boxplots of the objective function values obtained for the memristive system using six optimization algorithms: g-EEFO, EEFO, AOO, DOA, MO, and WO. The proposed g-EEFO exhibits the most compact distribution with the lowest median value, demonstrating highly stable and accurate convergence. In contrast, EEFO shows a slightly wider spread due to the absence of the global-best guidance mechanism. The remaining algorithms—AOO, DOA, MO, and WO—display substantially larger variances and higher medians, indicating reduced optimization precision. Among these, MO and DOA perform notably worse, with objective function values remaining several orders of magnitude higher.

Table 8 presents the statistical results of the parameter estimation task for the memristive system using six optimization algorithms: g-EEFO, EEFO, AOO, DOA, MO, and WO. The metrics reported include the best, worst, average, and standard deviation (SD) of the objective function values obtained from 20 independent runs. As seen in the table, the proposed g-EEFO algorithm achieves the lowest best, worst, and average objective

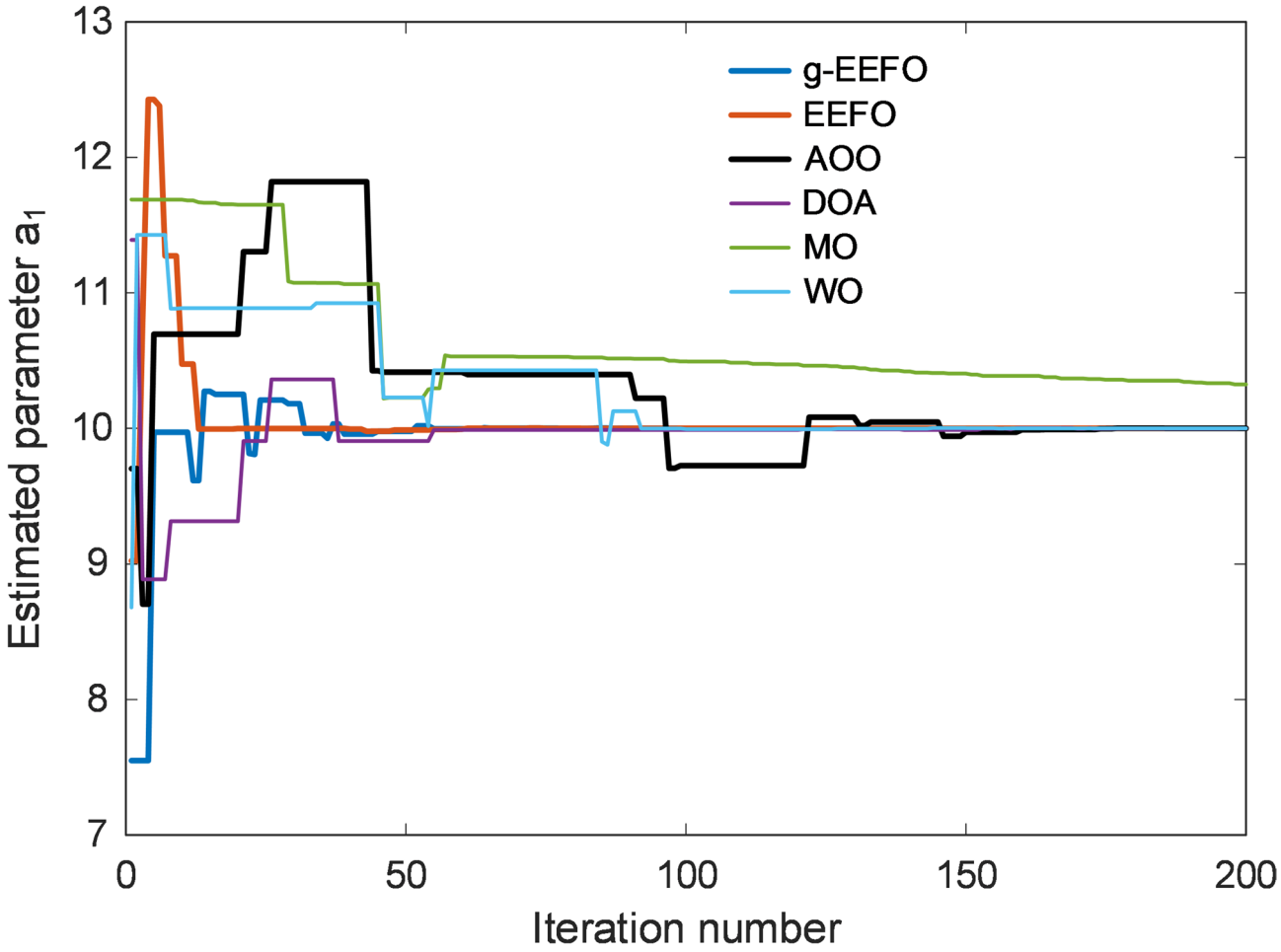

Fig. 9. Optimization curve of parameter a_1 for Lorenz system.

function values, accompanied by the smallest standard deviation (7.3458E − 13). The data substantiates a high degree of optimization precision and noteworthy operational resilience across independent runs. Conversely, competing methodologies, specifically MO and DOA, were characterized by substantially elevated mean errors and considerable standard deviations. This outcome reflects their inferior search efficacy and compromised convergence reliability.

Table 9 summarizes the Mann–Whitney U-test results comparing the proposed g-EEFO with five competing metaheuristic algorithms on the memristive chaotic system. All p-values are far below the significance level ($\alpha = 0.05$), indicating that the performance differences between g-EEFO and the other algorithms are statistically significant. The decision variable $h = 1$ in every comparison confirms the rejection of the null hypothesis, meaning the algorithms do not perform equivalently. In all cases, g-EEFO is identified as the superior method, supporting earlier findings from the objective function and boxplot analyses. These results demonstrate that the global-best guidance mechanism significantly enhances the EEFO framework, enabling more accurate and reliable parameter estimation for the memristive chaotic system.

Table 10 provides a comparative analysis of the performance of six optimization algorithms—g-EEFO, EEFO, AOO, DOA, MO, and WO—on the parameter identification task for the memristive chaotic system. The evaluation is based on the lowest MSE achieved by each algorithm and the corresponding estimated parameter values for the four system parameters a_1, a_2, a_3 and a_4. The goal is to minimize MSE while producing parameter estimates that closely match the true values of the memristive system ($a_1 = 1$, $a_2 = 1/3$, $a_3 = 0.6$, $a_4 = 1.5$). The proposed g-EEFO algorithm achieves the best overall performance, recording an extremely low MSE of 8.1850E − 19, which is several orders of magnitude smaller than its competitors. This exceptionally small error indicates that g-EEFO models the underlying dynamics of the memristive system with near-perfect accuracy. The corresponding parameter estimates produced by g-EEFO match the true values almost exactly, with all four parameters aligning closely to their theoretical targets and achieving the highest numerical precision. The EEFO algorithm provides the second-best performance with an MSE of 8.3415E − 15. Although its error is higher than that of g-EEFO, it still lies in a logarithmic range significantly smaller than those of AOO, DOA, WO, and especially MO. EEFO's parameter estimates are also highly accurate, showing deviations only in the lower decimal places. The algorithms AOO, DOA, and WO demonstrate moderate performance with MSE values ranging from 10^{-10} to 10^{-7}. While these values are far less precise than those of g-EEFO and EEFO, the

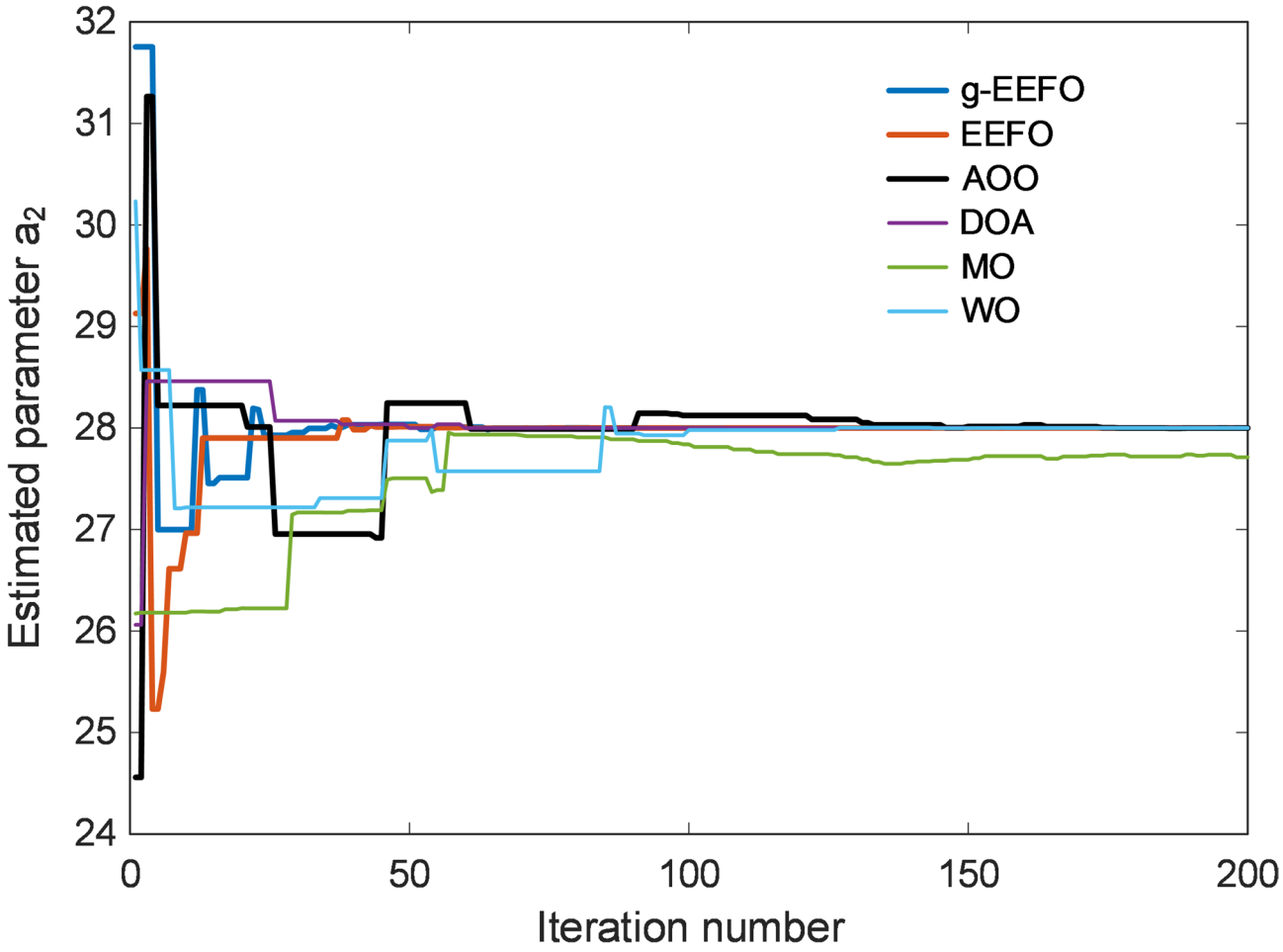

Fig. 10. Optimization curve of parameter a_2 for Lorenz system.

corresponding parameter estimates remain reasonably close to the true values, though noticeable deviations emerge—particularly for parameters a_1 and a_4..

The MO algorithm performs the worst, yielding a considerably larger MSE of 1.8897E – 04, which is several orders of magnitude higher than all other methods. This high error is reflected in its parameter estimates, which deviate substantially from the true values (e.g., $a_1 = 1.0923$, $a_2 = 0.3100$, $a_3 = 0.4225$, $a_4 = 1.6017$). Such discrepancies indicate that MO fails to capture the dynamical structure of the memristive system and converges to inaccurate parameter sets. Overall, the results clearly demonstrate that g-EEFO provides the highest estimation accuracy and reliability for the memristive chaotic system, outperforming all competing algorithms both in terms of MSE and parameter fidelity.

Table 11 presents the parameter estimation error rates of six optimization algorithms applied to the memristive chaotic system. The results demonstrate that g-EEFO achieves the lowest error rates across all four parameters, with values on the order of 10^{-6}% or lower, indicating near-perfect estimation accuracy. EEFO follows with slightly higher but still small errors, remaining well below 10^{-4}% for all parameters. In contrast, AOO and DOA exhibit moderate error levels, reaching up to 10^{-2}% and 10^{-1}%, respectively, suggesting reduced estimation precision. MO and WO show the worst performance, with error rates rising to several percent—particularly for parameters a_3 and a_4—indicating significant deviations from the true parameter values. Overall, the results confirm the clear superiority of g-EEFO in accurately identifying the memristive system parameters.

Figure 14 shows the convergence curves of six optimization algorithms for parameter identification of the memristive chaotic system. Among all methods, the proposed g-EEFO exhibits the fastest and most stable reduction in the MSE objective value. Its curve steadily decreases across the entire iteration range and reaches the lowest error level, demonstrating both strong global search ability and high-precision local refinement. EEFO follows a similar but noticeably slower trend, resulting in higher final error values. This difference highlights the effectiveness of the global-best learning mechanism added in g-EEFO. In contrast, AOO, DOA, MO, and WO show substantially weaker convergence behavior. Their curves flatten early, remain several orders of magnitude above g-EEFO, and reveal limited capability in escaping local minima. AOO performs moderately but still fails to match the high accuracy achieved by g-EEFO and EEFO. Overall, the results clearly indicate that g-EEFO provides the most accurate and reliable convergence performance for parameter estimation of the memristive chaotic system.

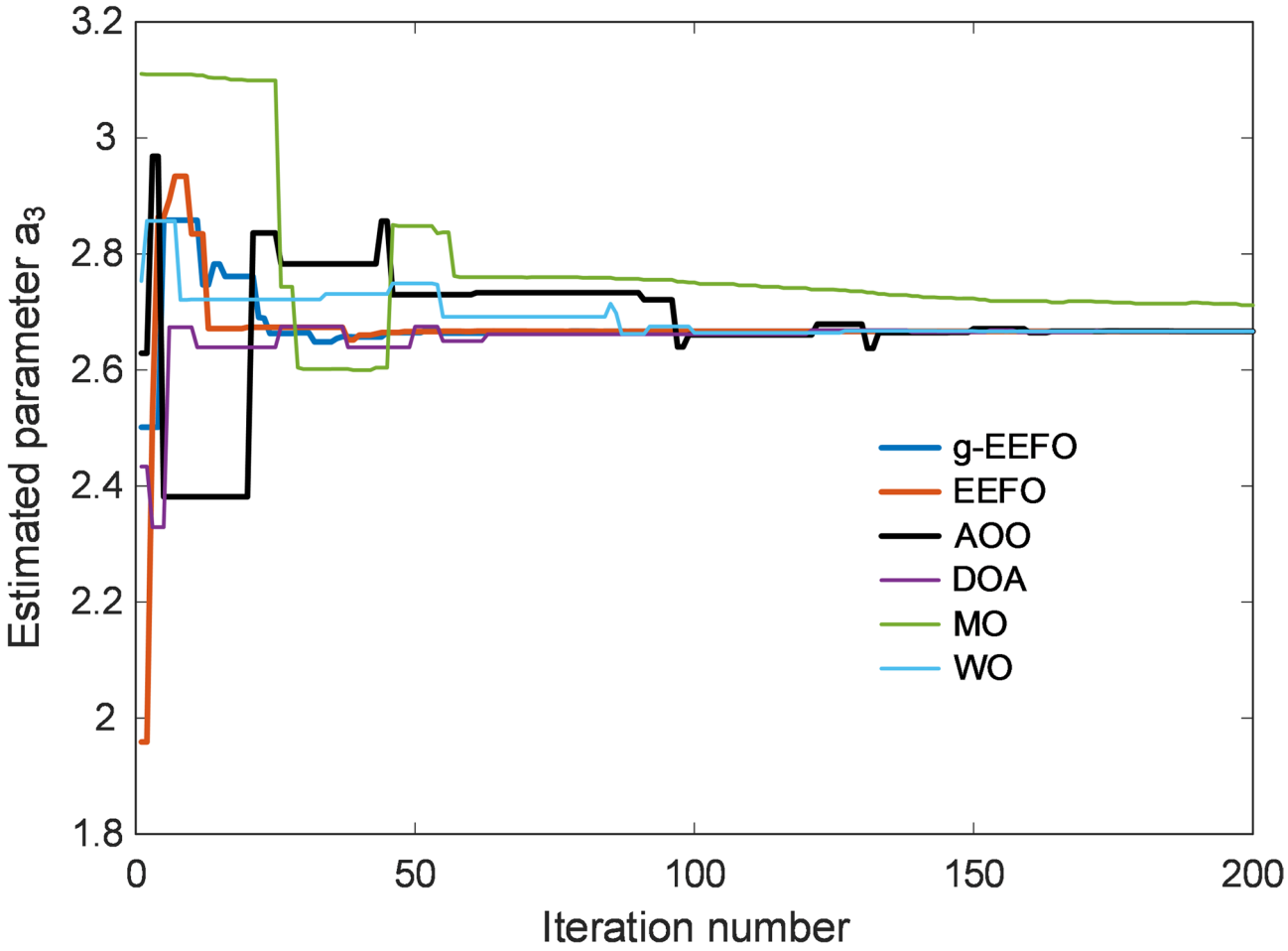

Fig. 11. Optimization curve of parameter a_3 for Lorenz system.

Figures 15, 16, 17 and 18 illustrate the parameter-evolution curves of the four memristive system parameters (a_1 - a_4) over 200 iterations for six optimization algorithms: g-EEFO, EEFO, AOO, DOA, MO, and WO. Across all parameters, the proposed g-EEFO consistently demonstrates the fastest and most stable convergence behavior. The estimated trajectories produced by g-EEFO rapidly settle to the true parameter values and exhibit minimal oscillation, confirming the algorithm's high estimation accuracy and strong robustness against stochastic fluctuations.

In contrast, the competing algorithms show considerably less stable convergence patterns. EEFO provides moderate stability but still displays small fluctuations and delayed convergence due to the absence of the global-best guidance mechanism. AOO and WO exhibit larger deviations and oscillatory behavior, indicating weaker exploitation capability. The DOA and MO algorithms demonstrate the poorest performance, with slow convergence and persistent divergence tendencies, especially in the estimation of parameters a_3 and a_4. Overall, the parameter-evolution curves reinforce the conclusion that g-EEFO provides superior convergence reliability and estimation precision for the memristive chaotic system. Its ability to maintain stable trajectories across all parameters highlights the effectiveness of integrating global-best learning into the EEFO framework.

Computational time analysis

In addition to convergence accuracy and stability, the practical efficiency of a metaheuristic algorithm is strongly influenced by its computational cost. To provide a clear assessment of runtime behavior, the average elapsed time per independent run is reported for all compared algorithms in Table 12 for both chaotic systems. Table 12 shows that the proposed g-EEFO requires only a marginally higher runtime than the baseline EEFO, with an increase of approximately 4–6% in both test systems. This overhead stems from the post-behavioral global-best modulation, which introduces a single vector update per individual and iteration. Importantly, this cost remains negligible when compared to the dominant expense of chaotic system simulation and fitness evaluation.

At the same time, g-EEFO remains consistently faster than AOO, MO, and WO, and is comparable to DOA. This indicates that the incorporation of global guidance does not impose a prohibitive computational burden. Instead, the slight increase in per-iteration cost is compensated by a substantial reduction in random drift and unproductive exploration, enabling the algorithm to reach high-quality regions of the search space more efficiently. These results confirm that the performance gains of g-EEFO are not achieved at the expense

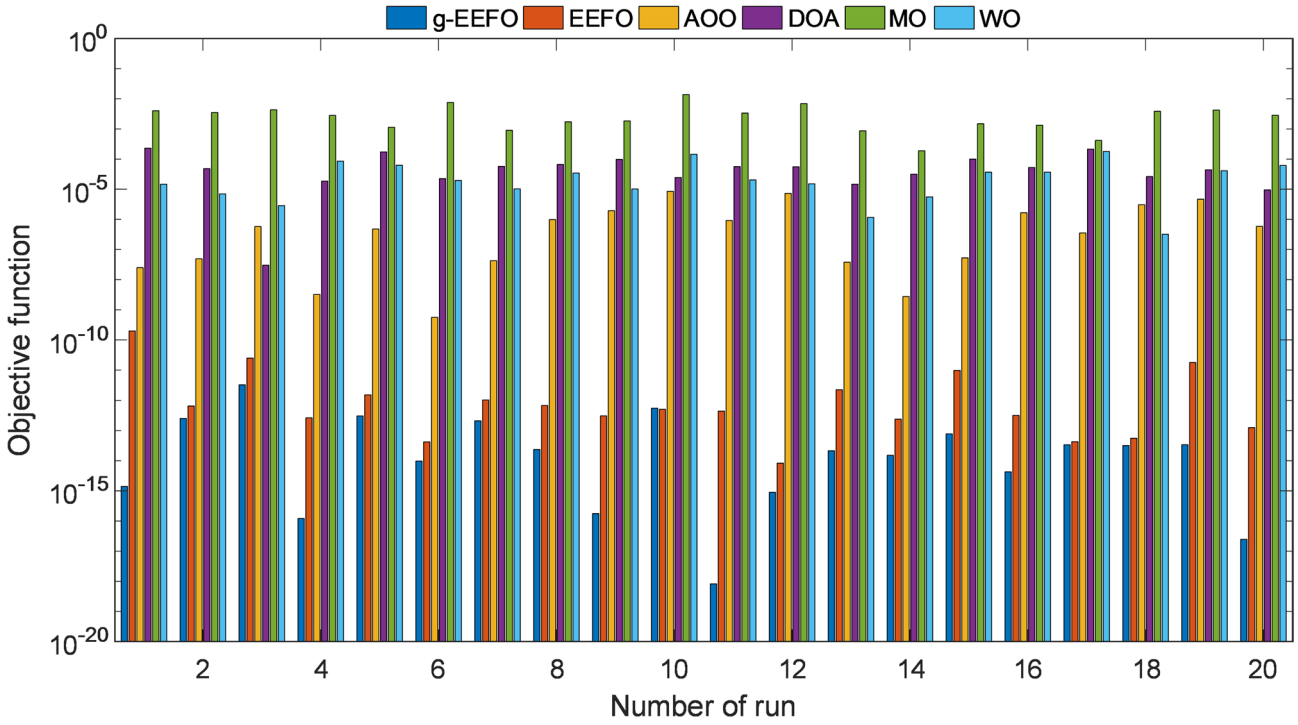

Fig. 12. Objective function values of six algorithms (g-EEFO, EEFO, AOO, DOA, MO, and WO) over 20 independent runs for the memristive system.

of impractical runtime. On the contrary, the proposed framework maintains a favorable balance between computational cost and optimization effectiveness, making it suitable for chaotic identification tasks where repeated numerical integration constitutes the dominant workload.

Comparison with reported studies

Tables 13 and 14 present a comparative assessment of the proposed g-EEFO algorithm against a set of well-established optimization methods previously reported in the literature for parameter estimation of the Lorenz and memristive chaotic systems. The results in Table 13 demonstrate that g-EEFO achieves a significantly lower MSE value (7.0213E − 26) compared to all reference algorithms, including evolutionary programming (EP)[52], improved version of cuckoo search (OLCS)[53], particle swarm optimization with ant colony optimization (PSO-ACO)[13], and starfish optimization algorithm (SFOA)[54]. Moreover, g-EEFO successfully identifies the system parameters (a_1, a_2, a_3) with perfect numerical accuracy, matching the theoretical values exactly. The competing algorithms, although achieving reasonably good approximations, show slight deviations—particularly in EP and OLCS—indicating less effective convergence characteristics compared to g-EEFO. These findings confirm the superiority of the proposed method in handling the complex nonlinear dynamics of the Lorenz system.

Similarly, Table 14 highlights the performance of g-EEFO for the memristive chaotic system in comparison with sine pareto sparrow search algorithm (SPSSA)[48], artificial bee colony algorithm (ABC)[48], fractional-order chaotic pareto pelican optimization algorithm (FPPOA)[55], and grey wolf optimizer (GWO)[55]. The proposed algorithm once again yields the best performance with an extremely low MSE value (8.1850E − 19), surpassing all reported methods by several orders of magnitude. Furthermore, the estimated parameters (a_1, a_2, a_3, a_4) are precisely aligned with the true system values, whereas the reference algorithms exhibit noticeable deviations, particularly in parameters a_3 and a_4, reflecting reduced estimation accuracy. The comparative results clearly indicate that g-EEFO offers superior robustness, accuracy, and stability in parameter estimation tasks for both classical and memristive chaotic systems.

Conclusion and future research directions

This study introduced the g-EEFO and demonstrated its effectiveness for parameter identification in chaotic dynamical systems. By embedding a behavior-aware, energy-regulated global learning mechanism into the ecological structure of EEFO, the proposed variant fundamentally reshapes the search dynamics of the original algorithm. The resulting framework preserves the stochastic richness and diversity of eel foraging while introducing coherent population-level guidance during exploitation. Extensive numerical investigations on two representative chaotic models (the classical Lorenz system and a structurally richer memristive chaotic system) confirm the clear advantages of g-EEFO. For the Lorenz system, g-EEFO achieves a best mean squared error on the order of 10^{-26}, outperforming all competing algorithms by several orders of magnitude and

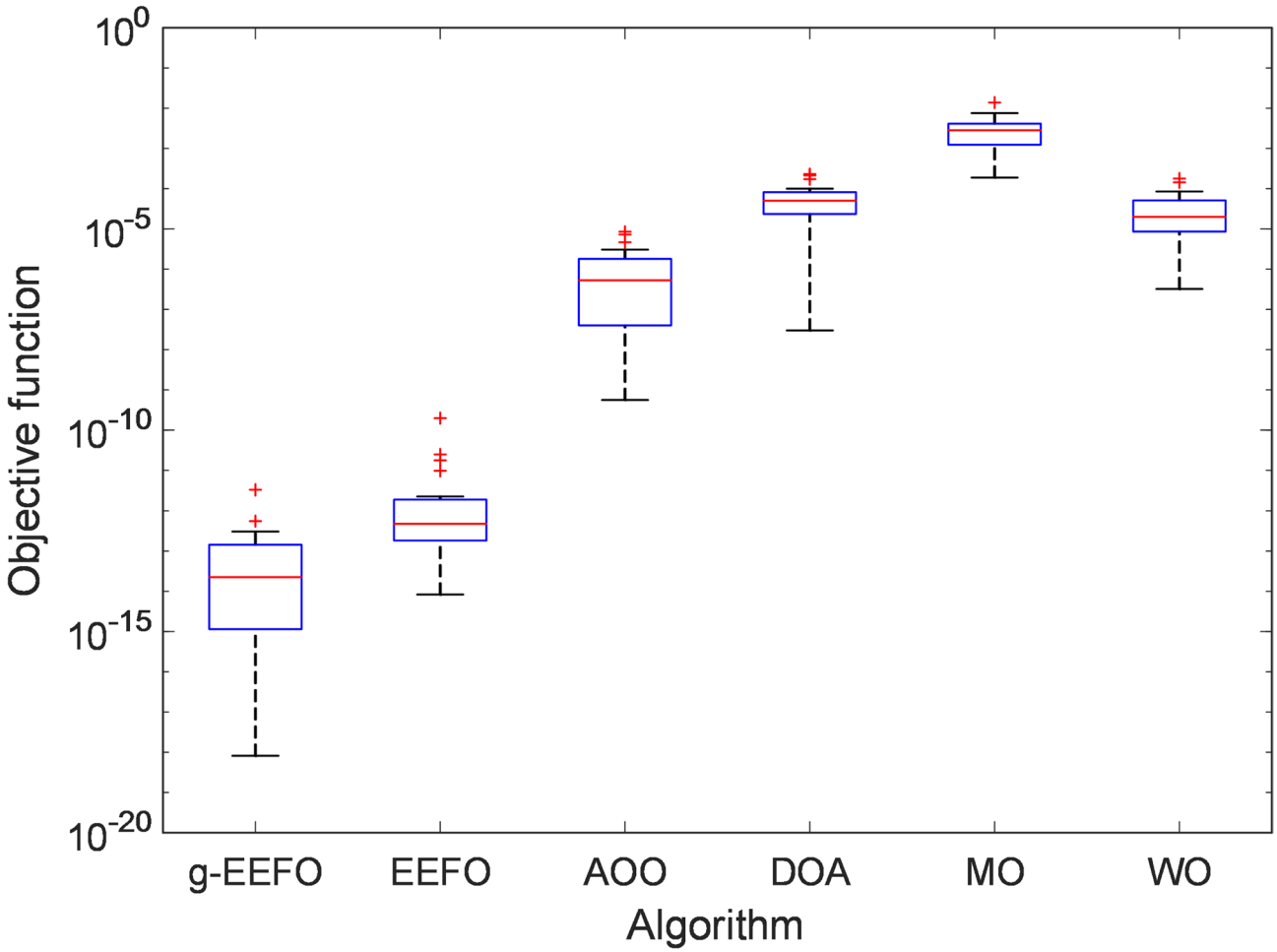

Fig. 13. Comparative boxplots of the objective function values obtained for the memristive system.

Algorithm	Best	Worst	Average	SD
g-EEFO	8.1850E−19	3.3052E−12	2.4428E−13	7.3458E−13
EEFO	8.3415E−15	1.9857E−10	1.2973E−11	4.4190E−11
AOO	5.6126E−10	8.5024E−06	1.5623E−06	2.4834E−06
DOA	3.0047E−08	2.3123E−04	6.7191E−05	6.5964E−05
MO	1.8897E−04	1.3863E−02	3.3694E−03	3.1840E−03
WO	3.2222E−07	1.7913E−04	3.9499E−05	4.8082E−05

Table 8. Statistical comparison of optimization algorithms for memristive system parameter estimation.

Algorithm	*p*-value	h	Winner
g-EEFO versus EEFO	1.0373E−04	1	g-EEFO
g-EEFO versus AOO	6.7956E−08	1	g-EEFO
g-EEFO versus DOA	6.7956E−08	1	g-EEFO
g-EEFO versus MO	6.7956E−08	1	g-EEFO
g-EEFO versus WO	6.7956E−08	1	g-EEFO

Table 9. Comparative Mann-Whitney U-test results for memristive chaotic system.

Algorithm	Best MSE	a_1	a_2	a_3	a_4
g-EEFO	8.1850E−19	1.000000006013	0.333333331185	0.599999986803	1.500000010481
EEFO	8.3415E−15	0.999999604051	0.333333431658	0.600000256048	1.499999888409
AOO	5.6126E−10	0.999953774133	0.333331391496	0.600292500883	1.500065450388
DOA	3.0047E−08	1.001588036768	0.332748350884	0.599172903803	1.503698273073
MO	1.8897E−04	1.092355280861	0.309971976985	0.422486097545	1.601725135094
WO	3.2222E−07	0.994040247288	0.335746351943	0.606048922135	1.487213624053

Table 10. Comparative best MSE values and estimated parameters of memristive system.

Algorithm	$Error\_rate = \frac{\lvert Actual - Estimation \rvert}{\lvert Actual \rvert} \times 100$			
	a_1	a_2	a_3	a_4
g-EEFO	6.0134E−07%	6.4464E−07%	2.1995E−06%	6.9871E−07%
EEFO	3.9595E−05%	2.9497E−05%	4.2675E−05%	7.4394E−06%
AOO	4.6226E−03%	5.8255E−04%	4.8750E−02%	4.3634E−03%
DOA	1.5880E−01%	1.7549E−01%	1.3785E−01%	2.4655E−01%
MO	9.2355%	7.0084%	2.9586E+01%	6.7817%
WO	5.9598E−01%	7.2391E−01%	1.0082%	8.5243E−01%

Table 11. Parameter Estimation error rates of six optimization algorithms for the memristive system.

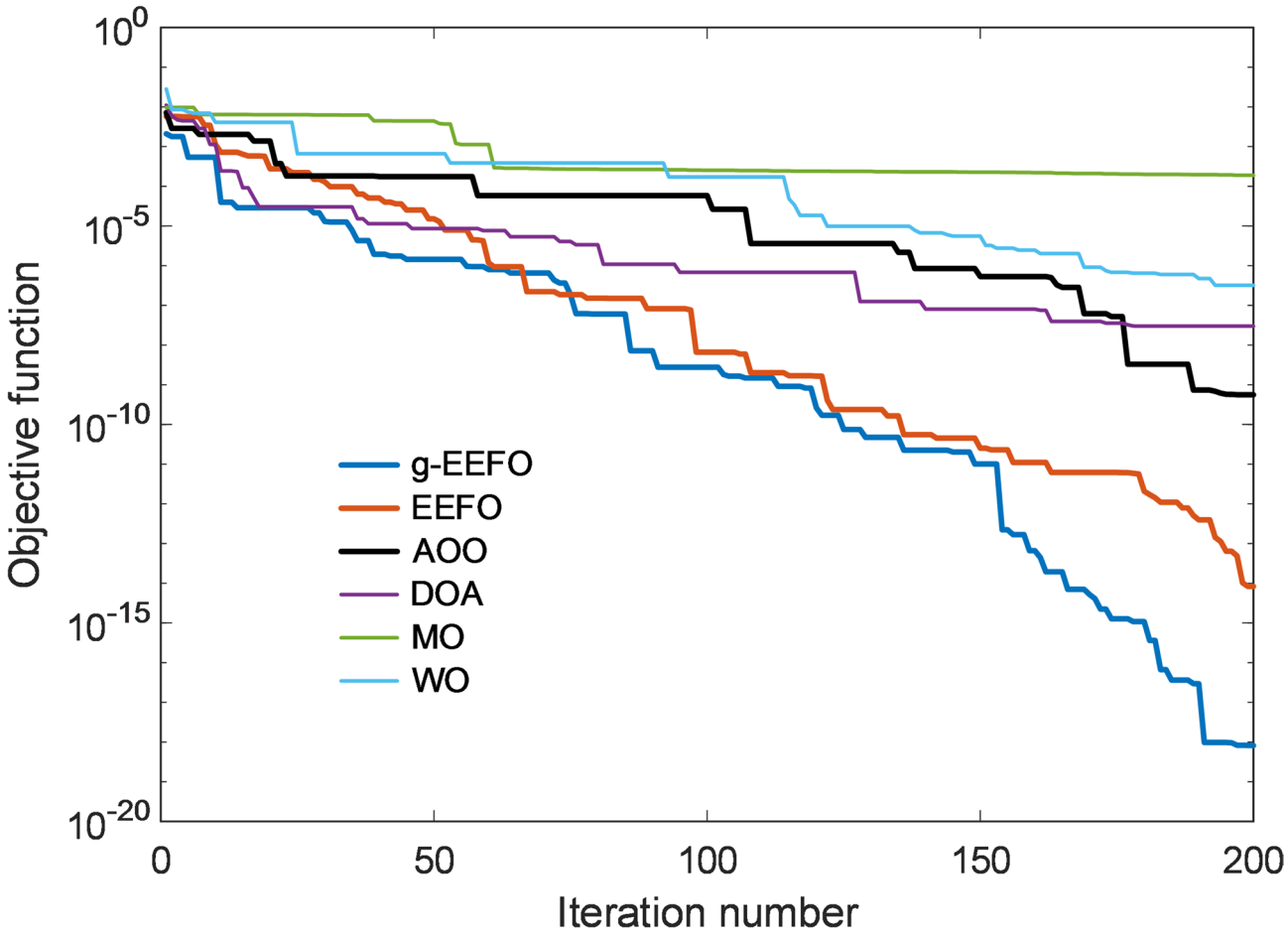

Fig. 14. Convergence curve of MSE objective function for memristive chaotic system.

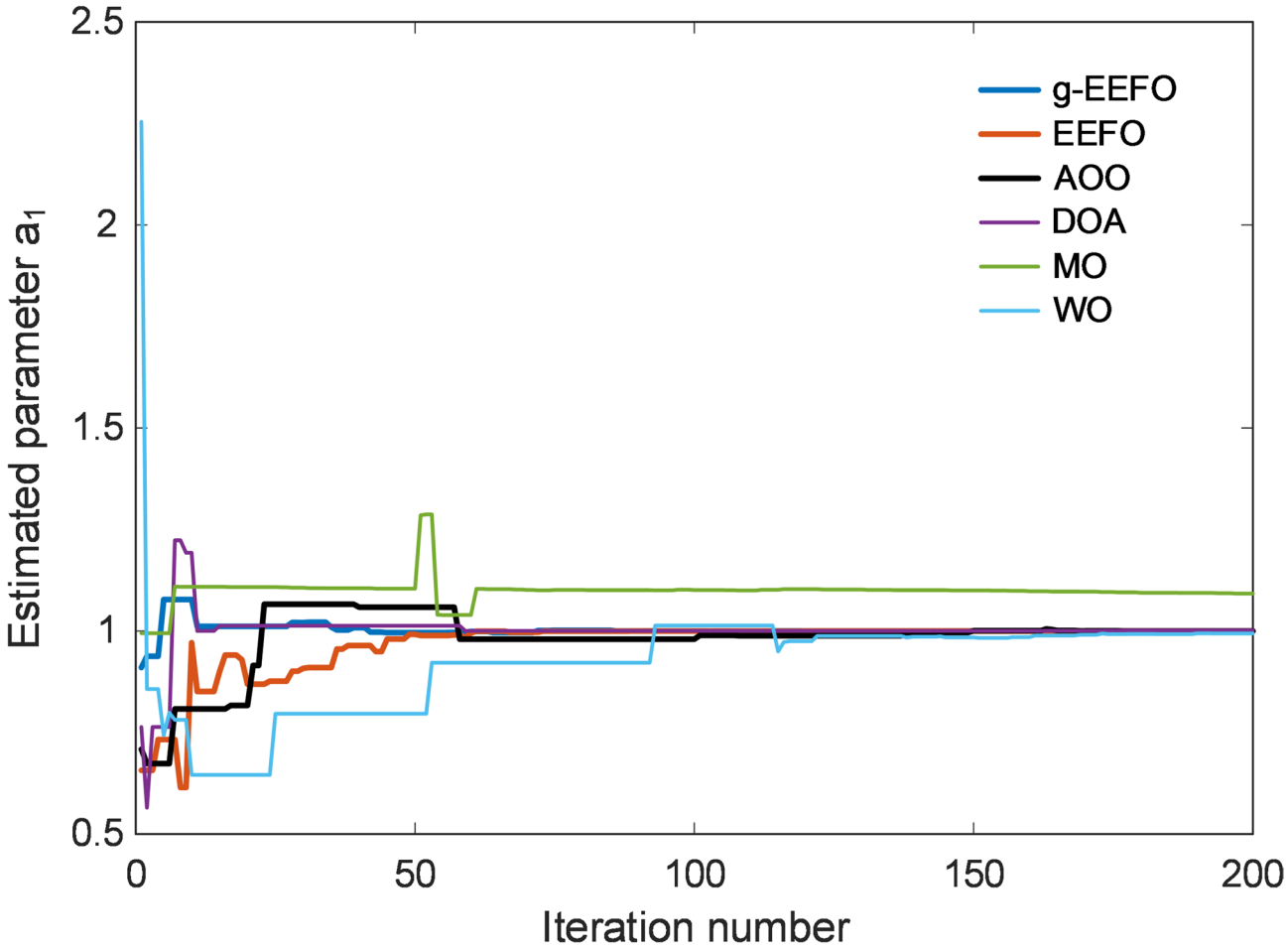

Fig. 15. Optimization curve of parameter a_1 for memristive system.

exhibiting an exceptionally small standard deviation across 20 independent runs. For the memristive system, similarly decisive gains are observed, with g-EEFO reaching error levels around 10^{-19} and maintaining the highest run-to-run stability. In both cases, the estimated parameters converge to their true values with near-perfect numerical precision. Convergence curves and parameter-evolution trajectories further demonstrate that g-EEFO reaches high-quality solutions faster and more reliably than both the baseline EEFO and other state-of-the-art metaheuristics. These results provide strong evidence that the proposed behavior-aware global guidance not only accelerates convergence but also enhances numerical accuracy and robustness in highly multimodal and chaotic landscapes. Unlike classical global-best-driven algorithms, which often suffer from premature convergence, g-EEFO maintains diversity through its phase-dependent, post-behavioral modulation, enabling sustained exploration in early stages and coherent exploitation in later phases. The main contributions of this study can be summarized as follows:

- A novel g-EEFO is proposed, in which global learning is embedded as a soft, behavior-aware modulation rather than as a dominant attractor.
- For the first time, EEFO and its improved form are applied to chaotic system parameter identification.
- A unified mathematical formulation is introduced to formalize the integration of global-best guidance into the EEFO behavioral cycle.
- Comprehensive experiments on two distinct chaotic systems demonstrate that g-EEFO achieves orders-of-magnitude improvements in accuracy, convergence speed, and statistical stability over existing metaheuristics.
- The proposed framework is shown to be model-agnostic and suitable for a broad class of chaotic and nonlinear identification problems.

Despite these encouraging results, several limitations warrant attention. First, validation is confined to two chaotic systems; although they represent different levels of complexity, further studies on higher-dimensional, fractional-order, and hyperchaotic models are needed to fully assess scalability. Second, computational cost increases with problem dimensionality and data length, which may restrict real-time applicability. Third, all algorithmic parameters are fixed; adaptive or self-tuning strategies may further enhance robustness. Finally, the study is purely numerical, and no real-time or hardware-in-the-loop experiments are considered. Future

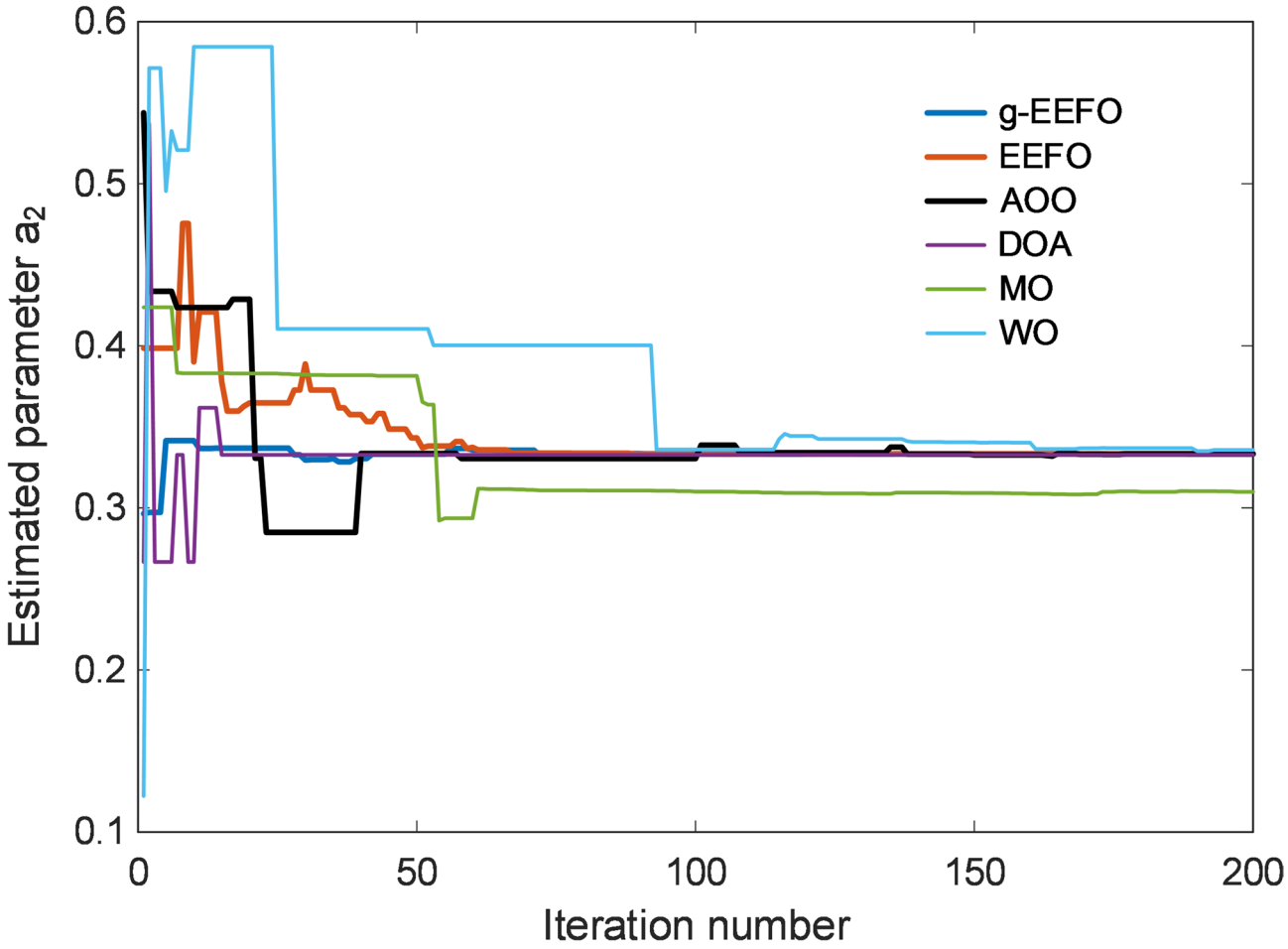

Fig. 16. Optimization curve of parameter a_2 for memristive system.

research may therefore focus on extending g-EEFO to hyperchaotic and fractional-order systems, developing adaptive parameter control mechanisms, and exploring real-time implementations in embedded and control-oriented environments. A particularly promising direction is the integration of lightweight surrogate or machine-learning models into the g-EEFO loop. In such a hybrid framework, data-driven regressors could be trained online to approximate the objective function and pre-screen candidate solutions generated by EEFO behaviors, allowing only the most promising individuals to be evaluated by the true physical model. This strategy would preserve the ecological and global-learning structure of g-EEFO while significantly reducing computational cost, especially in high-dimensional or long-horizon simulations. Together, these directions would further strengthen the practical relevance of the proposed framework for nonlinear system reconstruction and intelligent control.

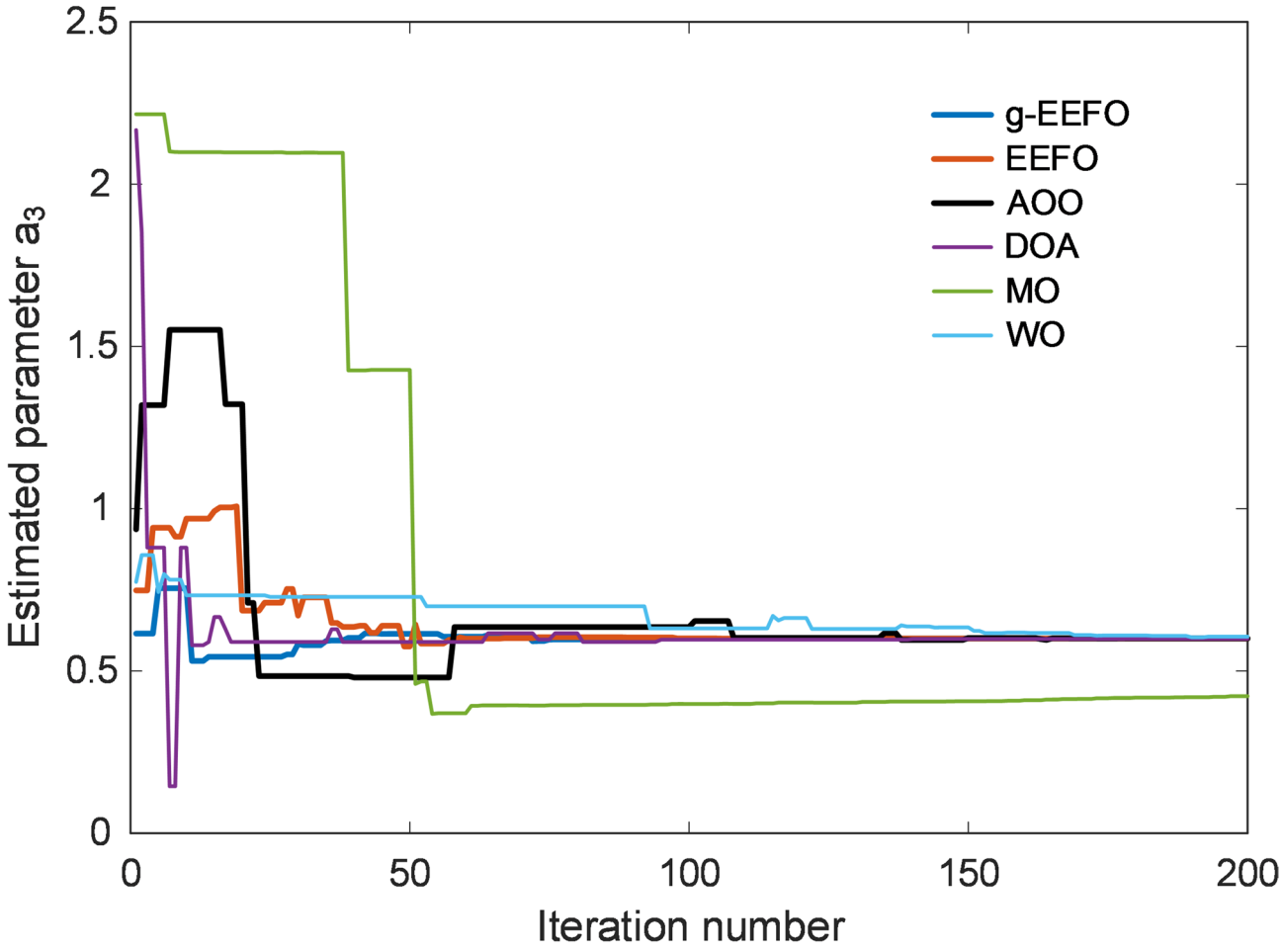

Fig. 17. Optimization curve of parameter a_3 for memristive system.

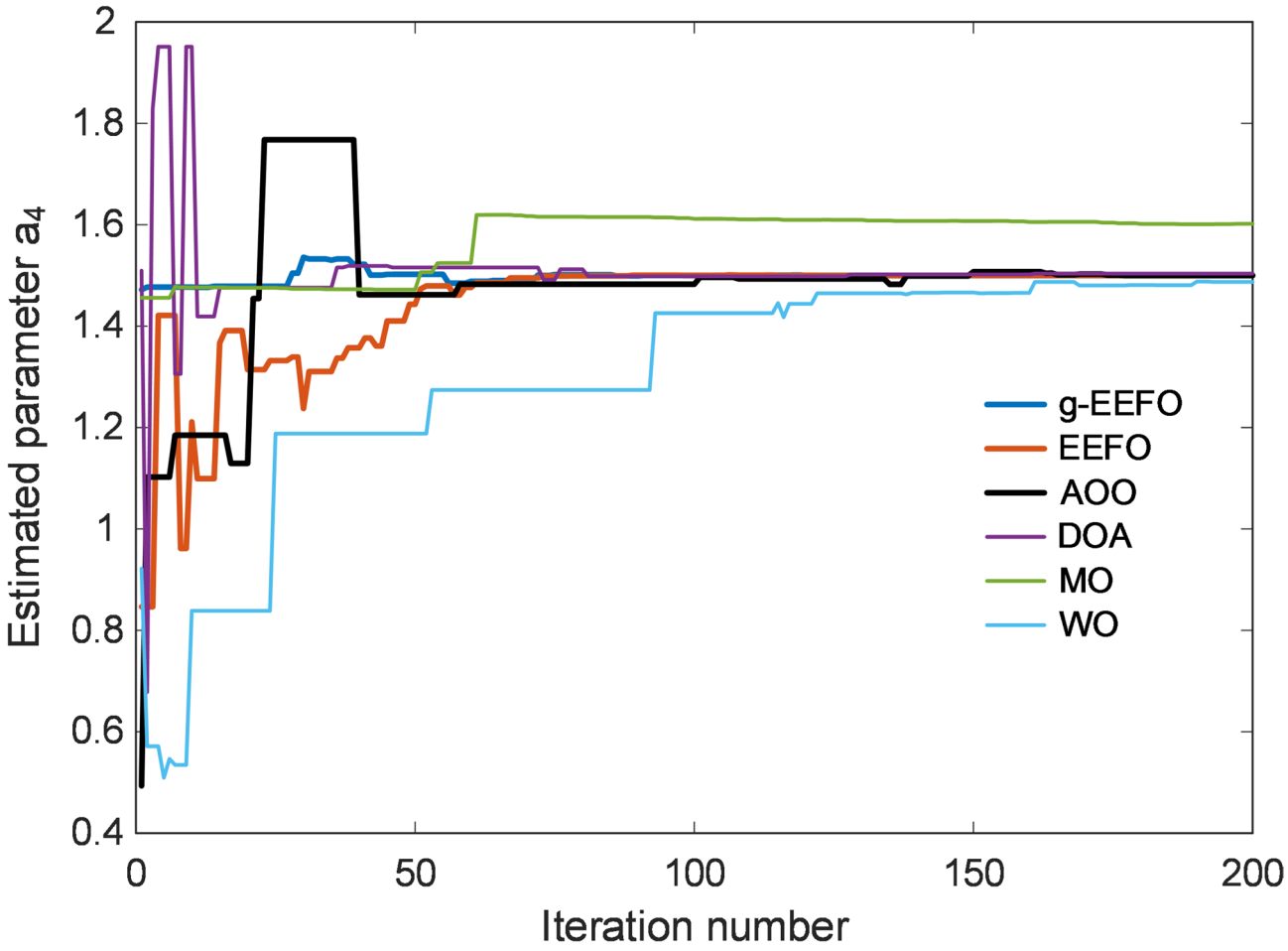

Fig. 18. Optimization curve of parameter a_4 for memristive system.

Test system	g-EEFO	EEFO	AOO	DOA	MO	WO
Lorenz chaotic system	26.3457	25.2920	36.3517	29.5054	31.0924	31.9236
Memristive chaotic system	25.0450	23.9338	34.4116	28.1973	29.5243	30.3389

Table 12. Elapsed times required by g-EEFO, EEFO, AOO, DOA, MO and WO algorithms.

Algorithm	Reference	Best MSE	a_1	a_2	a_3
g-EEFO	Proposed	7.0213E – 26	10.0000	28.0000	2.6667
EP	[52]	1.72E – 02	10.0162	27.9961	2.6659
OLCS	[53]	1.35E – 07	10.0000	28.0000	2.6667
PSO–ACO	[13]	1.03E – 06	10.0000	28.0000	2.6666
SFOA	[54]	1.64E – 15	10.0000	28.0000	2.6667

Table 13. Comparison of reported optimal parameter Estimation algorithms for Lorenz chaotic system.

Algorithm	Reference	Best MSE	a_1	a_2	a_3	a_4
g-EEFO	Proposed	8.1850E − 19	1.0000	0.3333	0.6000	1.5000
SPSSA	[48]	5.6200E − 03	0.9982	0.3342	0.6014	1.4953
ABC	[48]	5.6702E − 03	1.0016	0.3213	0.6507	1.5913
FPPOA	[55]	2.814E − 03	0.9952	0.3351	0.5989	1.4909
GWO	[55]	2.883E − 03	0.9905	0.3367	0.5723	1.4680

Table 14. Comparison of reported optimal parameter Estimation algorithms for memristive chaotic system.

Data availability

All related data are presented within the manuscript.

Received: 29 November 2025; Accepted: 6 February 2026
Published online: 12 February 2026

References

1. Modares, H., Alfi, A. & Fateh, M. M. Parameter identification of chaotic dynamic systems through an improved particle swarm optimization. *Expert Syst. Appl.* **37**, 3714 (2010).
2. Wang, L., Xu, Y. & Li, L. Parameter identification of chaotic systems by hybrid Nelder-Mead simplex search and differential evolution algorithm. *Expert Syst. Appl.* **38**, 3238–3245 (2011).
3. Deng, L. & Liu, S. A sine cosine algorithm guided by elite pool strategy for global optimization. *Appl. Soft Comput.* **164**, 111946 (2024).
4. Deng, L. & Liu, S. Snow ablation optimizer: A novel metaheuristic technique for numerical optimization and engineering design. *Expert Syst. Appl.* **225**, 120069 (2023).
5. Deng, L. & Liu, S. A multi-strategy improved slime mould algorithm for global optimization and engineering design problems. *Comput. Methods Appl. Mech. Eng.* **404**, 115764 (2023).
6. Deng, L. & Liu, S. An enhanced slime mould algorithm based on adaptive grouping technique for global optimization. *Expert Syst. Appl.* **222**, 119877 (2023).
7. Deng, L. & Liu, S. Incorporating Q-learning and gradient search scheme into JAYA algorithm for global optimization. *Artif. Intell. Rev.* **56**, 3705–3748 (2023).
8. Deng, L., Liu, S. A. & Novel Hybrid Grasshopper optimization algorithm for numerical and engineering optimization problems. *Neural Process. Lett.* **55**, 9851–9905 (2023).
9. Deng, L. & Liu, S. Advancing photovoltaic system design: an enhanced social learning swarm optimizer with guaranteed stability. *Comput. Ind.* **164**, 104209 (2025).
10. Ahmadi, M. & Mojallali, H. Chaotic invasive weed optimization algorithm with application to parameter Estimation of chaotic systems. *Chaos Solitons Fractals*. **45**, 1108–1120 (2012).
11. Li, C., Zhou, J., Xiao, J. & Xiao, H. Parameters identification of chaotic system by chaotic gravitational search algorithm. *Chaos Solitons Fractals*. **45**, 539–547 (2012).
12. Lin, J. & Chen, C. Parameter Estimation of chaotic systems by an oppositional seeker optimization algorithm. *Nonlinear Dyn.* **76**, 509–517 (2014).
13. Lazzús, J. A., Rivera, M. & López-Caraballo, C. H. Parameter Estimation of Lorenz chaotic system using a hybrid swarm intelligence algorithm. *Phys. Lett. Sect. A: Gen. At. Solid State Phys.* **380**, 1164–1171 (2016).
14. Zhang, H. et al. Parameter Estimation of nonlinear chaotic system by improved TLBO strategy. *Soft comput.* **20**, 4965–4980 (2016).
15. Mousavi, Y. & Alfi, A. Fractional calculus-based firefly algorithm applied to parameter Estimation of chaotic systems. *Chaos Solitons Fractals*. **114**, 202–215 (2018).
16. Anh, H. P. H., Son, N. N. & Van Kien, C. Ho-Huu, V. Parameter identification using adaptive differential evolution algorithm applied to robust control of uncertain nonlinear systems. *Appl. Soft Comput. J.* **71**, 672–684 (2018).
17. Ding, Z. H., Lu, Z. R. & Liu, J. K. Parameters identification of chaotic systems based on artificial bee colony algorithm combined with cuckoo search strategy. *Sci. China Technol. Sci.* **61**, 417–426 (2017).
18. Turgut, M. S., Sağban, H. M., Turgut, O. E. & Özmen, Ö. T. Whale optimization and sine–cosine optimization algorithms with cellular topology for parameter identification of chaotic systems and Schottky barrier diode models. *Soft comput.* **25**, 1365–1409 (2021).
19. Nuñez-Perez, J. C. et al. Maximizing the chaotic behavior of fractional order Chen system by evolutionary algorithms. *Math. 2021*. **9**, 1194 (2021).
20. Zainel, Q. M., Darwish, S. M. & Khorsheed, M. B. Employing quantum fruit fly optimization algorithm for solving Three-Dimensional chaotic equations. *Math. 2022*. **10, Page 4147** (10), 4147 (2022).
21. Rizk-Allah, R. M., Farag, M. A., Barghout, M. H. & Hassanien, A. E. A Memory-Based particle swarm optimization for parameter identification of Lorenz chaotic system. *Lecture Notes Networks Syst.* **394**, 571–587 (2022).
22. Sattar, D. & Shehadeh Braik, M. Metaheuristic methods to identify parameters and orders of fractional-order chaotic systems. *Expert Syst. Appl* **228** (2023).
23. Kumar, K. Data-driven modeling and parameter estimation of nonlinear systems. *Eur. Phys. J. B* **96**, 1–13 (2023).
24. Nathasarma, R. & Roy, B. K. Physics-Informed Long-Short-Term memory neural network for parameters Estimation of nonlinear systems. *IEEE Trans. Ind. Appl.* **59**, 5376–5384 (2023).
25. Cavlak, Y., Ateş, A., Abualigah, L. & Elaziz, M. A. Fractional-order chaotic oscillator-based Aquila optimization algorithm for maximization of the chaotic with Lorentz oscillator. *Neural Comput. Appl.* **35**, 21645–21662 (2023).
26. Farjami, A. A. & Yaghoobi, M. Kardehi Moghaddam, R. Extended cascade chaotic systems and Estimation parameters with new chaotic grey Wolf algorithm. *J. Experimental Theoretical Artif. Intell.* **36**, 1187–1211 (2024).
27. Ahmadi, A. et al. A novel megastable chaotic system with hidden attractors and its parameter Estimation using the sparrow search algorithm. *Comput. 2024.* **12**, 245 (2024).
28. Wu, G. C., Wu, Z. Q. & Zhu, W. Data-driven discrete fractional chaotic systems, new numerical schemes and deep learning. *Chaos* **34** (2024).
29. Lin, K., Han, X., Xu, X., Zong, T. & Zhou, X. Parameter estimation of fractional-order chaotic system based on adaptive artificial evolutionary fish swarm algorithm. *Proceedings of IEEE 14th Data Driven Control and Learning Systems Conference, DDCLS 2025* 739–744 (2025). https://doi.org/10.1109/DDCLS66240.2025.11066043
30. Kumar, K. & Kostina, E. Machine learning in parameter Estimation of nonlinear systems. *Eur. Phys. J. B 2025*. **98:4 98**, 1–18 (2025).

31. Zhao, W. et al. Electric eel foraging optimization: A new bio-inspired optimizer for engineering applications. *Expert Syst. Appl* **238** (2024).
32. Mehta, P., Yildiz, B. S., Sait, S. M. & Yldlz, A. R. Optimization of electric vehicle design problems using improved electric eel foraging optimization algorithm. *Materialpruefung/Materials Test.* **66**, 1230–1240 (2024).
33. Abdelwahab, S. A. M. et al. Optimal control and optimization of Grid-Connected PV and wind turbine hybrid systems using electric eel foraging optimization algorithms. *Sens. 2024*. **24**, 2354 (2024).
34. Al-qaness, M. A. A. et al. Optimized quantum LSTM using modified electric eel foraging optimization for real-world intelligence engineering systems. *Ain Shams Eng. J.* **15**, 102982 (2024).
35. Ebrahim, M. A., Ragab, A. S., Aziz, B. A. & AbdelHadi, H. A. Electric Eel foraging optimization based control design of islanded microgrid. *Sci. Rep.* **15**, 1–22 (2025).
36. Rezk, H., Ghasemi, M., Al Saadi, A. & Sayed, E. T. Experimental validation of single and multi-objective optimization of microbial fuel cell based on recent electric eel foraging algorithm. *Energy* **339**, 138989 (2025).
37. Ekinci, S. Nonlinear controller design for automotive engine speed regulation utilizing electric eel foraging optimization. *Int J. Dyn. Control* **13** (2025).
38. Abdel-salam, M., Houssein, E. H., Emam, M. M., Abdel Samee, N. & Azam, M. T. A novel dynamic Nelder-based electric eel foraging algorithm for global optimization and pathological colorectal cancer image segmentation. *Comput. Biol. Med.* **197** (2025).
39. Mehmood, K. et al. Design of chaos induced Aquila optimizer for parameter estimation of electro-hydraulic control system. *Comput. Model. Eng. Sci.* **143**, 1809–1841 (2025).
40. Mehmood, K. et al. Design of chaotic young's double Slit experiment optimization heuristics for identification of nonlinear muscle model with key term separation. *Chaos Solitons Fractals*. **189**, 115636 (2024).
41. Wang, X. Gyro fireworks algorithm: A new metaheuristic algorithm. *AIP Adv.* **14** (2024).
42. Wang, X. Bighorn sheep optimization algorithm: a novel and efficient approach for wireless sensor network coverage optimization. *Phys. Scr.* **100**, 075230 (2025).
43. Wang, X. & Yao, L. Cape Lynx optimizer: A novel metaheuristic algorithm for enhancing wireless sensor network coverage. *Measurement* **256**, 118361 (2025).
44. Wang, R. et al. The animated oat optimization algorithm: A nature-inspired metaheuristic for engineering optimization and a case study on wireless sensor networks. *Knowl. Based Syst.* **318** (2025).
45. Lang, Y. & Gao, Y. Dream optimization algorithm (DOA): A novel metaheuristic optimization algorithm inspired by human Dreams and its applications to real-world engineering problems. *Comput Methods Appl. Mech. Eng* **436** (2025).
46. Yuan, Y. et al. Musk ox optimizer (MO): A novel optimization algorithm and its application. *Clust. Comput.* **28** (2025).
47. Han, M. et al. Walrus optimizer: A novel nature-inspired metaheuristic algorithm. *Expert Syst. Appl.* **239** (2024).
48. Xiong, Q., Shen, J., Tong, B. & Xiong, Y. Parameter identification for memristive chaotic system using modified sparrow search algorithm. *Front. Phys.* **10**, 912606 (2022).
49. Abualigah, L. et al. Optimized image segmentation using an improved reptile search algorithm with Gbest operator for multi-level thresholding. *Sci. Rep.* **15**, 1–45 (2025).
50. Lorenz, E. N. Deterministic nonperiodic flow. *J. Atmos. Sci.* **20**, 130–141 (1963).
51. McKnight, P. E., Najab, J., Mann-Whitney, U. & Test *Corsini Encycl. Psychol.* **1–1** https://doi.org/10.1002/9780470479216.CORPSY0524. (2010).
52. Chang, J. F., Yang, Y. S., Liao, T. L. & Yan, J. J. Parameter identification of chaotic systems using evolutionary programming approach. *Expert Syst. Appl.* **35**, 2074–2079 (2008).
53. Li, X. T. & Yin, M. H. Parameter Estimation for chaotic systems using the cuckoo search algorithm with an orthogonal learning method. *Chin. Phys. B* **21** (2012).
54. Ekinci, S., Turkeri, C., Izci, D., Kiselychnyk, O. & Gunes, B. B. Opposition-based starfish optimization algorithm for function optimization. *9th International Artificial Intelligence and Data Processing Symposium (IDAP)* 1–4 (2025).https://doi.org/10.1109/IDAP68205.2025.11222186
55. Xiong, Q., She, J. & Xiong, J. A. New pelican optimization algorithm for the parameter identification of memristive chaotic system. *Symmetry 2023*. **15**, 1279 (2023).

Author contributions

Davut Izci, Serdar Ekinci: Conceptualization, Methodology, Software, Visualization, Investigation, Writing-Original draft preparation, İrfan Ökten, Vedat Tümen, Burcu Bektaş Güneş, Mostafa Rashdan, Mohammad Salman: Data curation, Validation, Supervision, Resources, Writing - Review & Editing, Writing - Review & Editing.

Funding

This research received no specific grant from any funding agency in the public, commercial, or not-for-profit sectors.

Declarations

Competing interests

The authors declare no competing interests.

Additional information

Correspondence and requests for materials should be addressed to D.I.

Reprints and permissions information is available at www.nature.com/reprints.

Publisher's note Springer Nature remains neutral with regard to jurisdictional claims in published maps and institutional affiliations.